CHALMERS
UNIVERSITY OF TECHNOLOGY

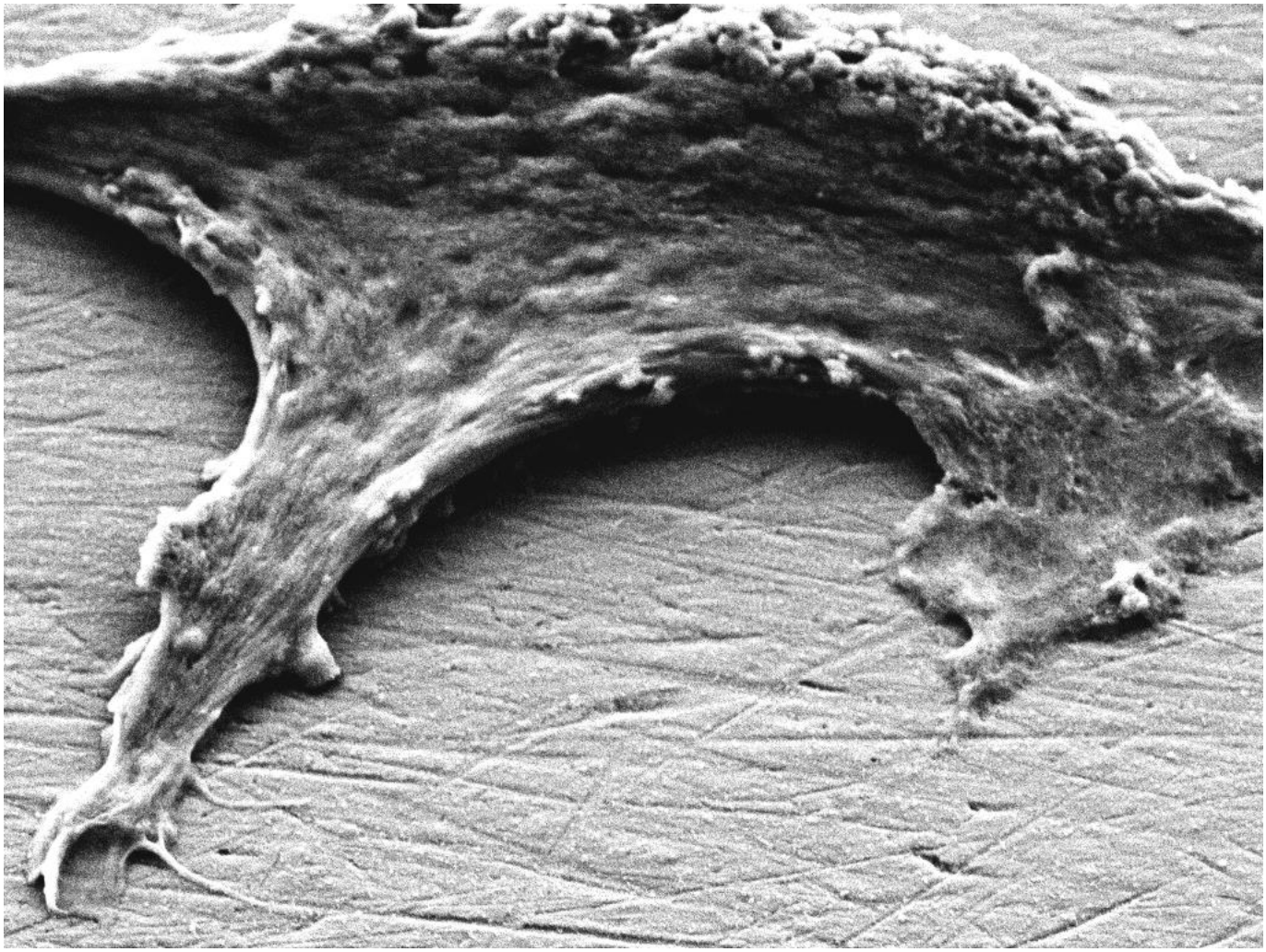

Promoting osseointegration in titanium implants using pulsed electrical stimulation

Master's thesis in Biomedical Engineering

EMILY PETTERSEN

DEPARTMENT OF ELECTRICAL ENGINEERING
CHALMERS UNIVERSITY OF TECHNOLOGY
Gothenburg, Sweden 2020
www.chalmers.se

DEPARTMENT OF ELECTRICAL ENGINEERGING
CHALMERS UNIVERSITY OF TECHNOLOGY
Gothenburg, Sweden
www.chalmers.se

Master Thesis

Promoting osseointegration in titanium implants using pulsed electrical stimulation

Emily Pettersen, emilyp@chalmers.se

August 18, 2020

CHALMERS
UNIVERSITY OF TECHNOLOGY

Promoting osseointegration in titanium implants using pulsed electrical stimulation

A master thesis project where the effect of pulsed electrical stimulation on osseointegration was investigated.

EMILY PETTERSEN

Supervisor and examiner: Dr Max Ortiz Catalan, Associate Professor,
Department of Electrical Engineering, Chalmers University of Technology

Department of Electrical Engineering
Chalmers University of Technology
SE-412 96 Gothenburg
Sweden
Telephone + 46 (0)31 – 772 1000

Cover: SEM image of an osteoblast attached to a Ti6AlV4 implant surface. Magnification 5000x, accelerating voltage 5 kV and working distance 3.8 mm.

Gothenburg, Sweden 2020

Acknowledgement

I would like to express my very great appreciation to my supervisor and examiner Associate Professor Max Ortiz Catalan for all supervision, commitment and support during the thesis work. I am particularly grateful for the supervision and assistance given by Dr Furqan Ali Shah during the designing phase, the performance of the in vitro study and help with the scanning electron microscopy images. I would also like to thank Dr Enzo Mastinu for all the help with the electrical stimulation part, including the coding and setup of the function and direct current stimulator. Special thanks for the initial discussion and materials given by Professor Julie Gold. My grateful thanks to Jurek Lamkiewicz for manufacturing the titanium parts.

I would also like to extend my thanks to the personnel at the department of Biomaterials at the Sahlgrenska Academy for their help in offering me their knowledge and resources in running the *in vitro* study. Lastly, I want to thank the whole Biomechantronics and Neurorehabilitation Laboratory group for supporting me and letting me be a part of their group.

Emily Pettersen, Gothenburg, August 2020

Abstract

Electrical stimulation has shown to be a potential approach for promoting osseointegration, where osseointegration defines the biological bonding between an implant surface and bone tissue. Inadequate osseointegration is one of the major factors of implant failure, which in the worst case leads to implant removal and shortening of the residual limb. Electrical stimulation has been tested in different models, both *in vitro* and *in vivo*, with various approaches ranging from different configurations to current sources and electrical stimulation parameters. However, optimal stimulation parameters have not been thoroughly investigated.

This thesis investigates the effect on osseointegration of pulsed electrical stimulation with similar properties as used in peripheral nerve stimulation to restore sensory feedback in artificial limbs. A literature review was conducted where previous work yielding positive and negative outcomes was analysed and summarised with respect to stimulation parameters. An *in vitro* model was then developed to further study a variety of stimulation parameters. This model was used to investigate five different conditions where Ti6Al4V implants were precultured with MC3T3-E1 cells and stimulated for 72 h. Stimulation pulses of 10, 20, and 50 μA were compared to each other and to a control group where no stimulation was applied. In addition, two different frequencies, 50 and 100 Hz, were also tested and compared to each other as well as to a non-stimulated group.

Pulsed electrical stimulation was found to have a beneficial impact on the potential promotion of osseointegration. Pulse amplitudes of 20 μA were found more advantageous compared to 10 and 50 μA, although no significant difference between the amplitude groups in cell proliferation was found, but 20 and 50 μA showed a significant higher increase in collagen production compared to 10 μA and non-stimulated surfaces. In addition, higher frequency, 100 versus 50 Hz, showed a significantly higher cell proliferation and production of collagen.

Keywords: osseointegration, pulsed electrical stimulation, osteoblast, *in vitro* model, prostheses, cell proliferation, collagen production

Contents

1 Introduction

The discovery of osseointegration, the natural phenomenon that defines the process of biological bonding in the environment between an implant surface and bone tissue [1], revolutionised the application of limb prostheses by providing the means to skeletal attachment [2] and thus allowing for mechanical coupling and load transfer [3]. The osseointegrated prosthesis has increased the quality of life for amputees by exceeding limitations with the conventional socket prosthesis such as skin irritations and nerve compression, and allowing for control of the artificial limb and restoration of sensory and tactile perception [4], [5]. It has been suggested that in order to obtain a successful osseointegrated prosthesis, the bone-implant interface must be achieved rapidly, be properly maintained, and remain free from infections [4].

Amongst metallic biomaterials, titanium and its alloys are most frequently used in load-bearing orthopaedic implants due to their biocompatibility properties, mechanical strength and high corrosion resistance [6], [7]. Despite titanium implant's well integration with surrounding bone tissue, there exist issues with this technique. Implants are regarded as osseointegrated when there is no progressive relative movement at the implant-bone interface [8], to achieve this condition it can take up to several months depending on the implant design and patient's bone quality. In conditions when early implant loading is desired, or when the implant is placed in weakened bone, there is a need to stimulate the osseointegration progression to a rapid and potentially better completion [9], [10]. Moreover, one of the major factors of implant failure is inadequate osseointegration [2]. In this scenario there is a substantial risk for bacteria attachment and biofilm formation at the implant surface which can emerge several years after the implantation [11], as well as implant loosening. Those conditions will in the worst case lead to implant removal which also requires shortening of the residual limb [12].

The concept of enhancing biofunctionality at the implant-bone interface for reducing healing time and increasing implant's lifespan has been investigated, developed and implemented with different engineering approaches such as development of different metal alloys and porous implants, as well as alteration of implant surface properties including coatings, roughness, charge etc. [6]. Electrical stimulation has been established and achieved value as a modality for clinical treatments of a wide spectrum of different disorders and disabilities [13]. Implants that deliver electrical stimulation are used in for example cochlear implants to regain hearing [14], wound-healing therapies to enclosure chronic wounds [15] and in prostheses applications to allow for control of the artificial limb as well as restoration of sensory and tactile perception [16]. The idea of using electrical stimulation with the purpose to promote osseointegration occurred several decades ago and has ever since been explored in different models, both *in vitro* and *in vivo*, with various approaches ranging from different electrode configurations to sources of current and electrical stimulation parameters. Many studies have received a significant increase in bone to implant contact [9] [6] [17] [18] [19], greater osteoblast function, e.g, differentiation of preosteoblasts [13] [20], and proliferation [21] by using electrical stimulation, which may have significant implications for promoting osseointegration. The underlying pathway in the occurrence of the enhanced osseointegration is yet undiscovered and the ideal electrical stimulation parameters with the greatest impact remains undefined [4].

1.1 Background

The background provides fundamental knowledge in the bone remodelling process and Integrum's e-OPRA implant system.

1.1.1 Bone Remodelling

Bone remodelling is a lifelong process where synthesis and destruction of bone matrix occurs continuously to maintain a fully functional bone tissue. Several bone remodelling events occurs simultaneously and independently throughout the whole body, resulting in a completely renewed skeleton every ten years [22]. The process gives bone its mature structure and it maintains the level of calcium in the body [23]. There are three main types of bone cells that are incorporated in the process of bone remodelling which originate from the mesenchymal stem cell, namely, osteoclasts, osteoblasts and osteocytes. The task for an osteocyte is to be a part of the destruction of bone, also called bone resorption. Osteoclasts release inorganic calcium into the bloodstream in order to meet a metabolic balance in the body, and simultaneously allow the inhibited bone structure to be reshaped into adult propositions [23].

The other main cell type in bone remodelling, the osteoblast, is a part of the bone formation in order to maintain skeletal structure. The osteoblast produces many cell products, including enzymes such as alkaline phosphates (ALP) and collagenase, hormones, multiple different growth factors and a complex dense fibril matrix of collagen, mainly collagen type 1. The osteoblast will continuously create bone matrix until it becomes surrounded of the matrix, and as the material calcifies it becomes trapped in a space called lacuna. When it is entrapped, the cell becomes an osteocyte [24]. Figure 1 visualises the different phases of the bone remodelling process where various cell types are incorporated in the different phases.

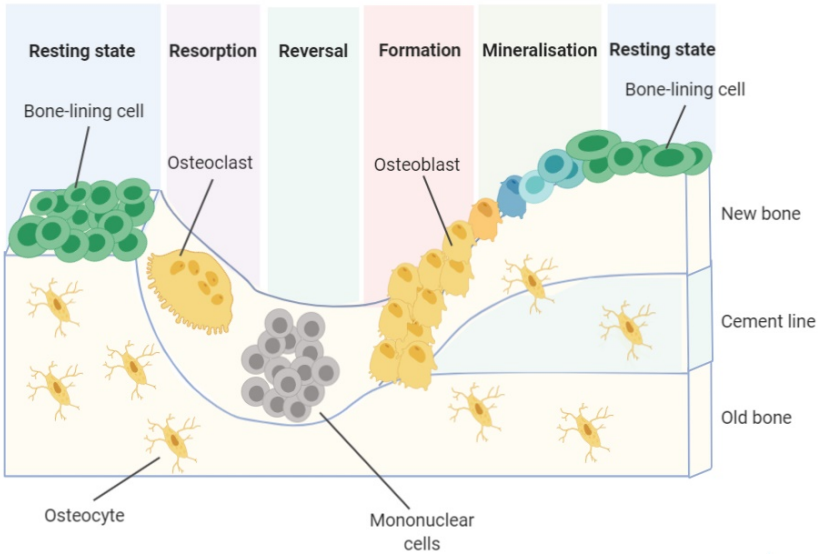

Figure 1: Bone remodelling process, with the different phases; resting state, resorption, reversal, formation, mineralisation, and lastly resting state once again. Various cell types are incorporated in the phases. Image reference: [25]

1.1.2 e-OPRA Implant System

In 1990, Prof. P.I. Brånemark and Prof. B. Rydevik performed the world's first surgery where a patient was implanted with a transfemoral osseointegrated prosthesis in Gothenburg, Sweden. In 1998 Intergum was founded by Prof. P.I. Brånemark and his son Prof. R. Brånemark, and in 1999 Intergum received their first CE marking for their OPRA implant system, (OPRA™, Osseointegrated Prostheses for the Rehabilitation of Amputee) [26]. Integrum have for more than two decades continued to develop, improve, and adapt their OPRA system to several parts of the body. They have achieved results along the way such as FDA approvement of the OPRA implant system for amputations above the knee and an updated version of OPRA to e-OPRA where permanently implanted neuromuscular electrodes are used to connect the prosthesis to the nervous system, thereby allowing the patient control of movements of the artificial limb and sensation [16] [27].

In the e-OPRA system, the artificial limb is attached to the abutment which in turn is connected to the osseointegrated Ti6Al4V fixture. This connection allows the load to be transferred from the prosthetic limb to the bone. The abutment is attached to the fixture via the abutment screw where a parallel connector is distally embedded at the end of the screw and linked to the electrical interface in the prosthetic limb. The connector is electrically connected to a second connector that is embedded in the proximal end of the screw. The stack connector is linked with several different connectors until it reaches the final connector which is located in the soft tissue. The neuromuscular electrodes are linked to the connector, where the electrical signals are transferred [28]. Figure 2 visualises the e-OPRA system with the different components.

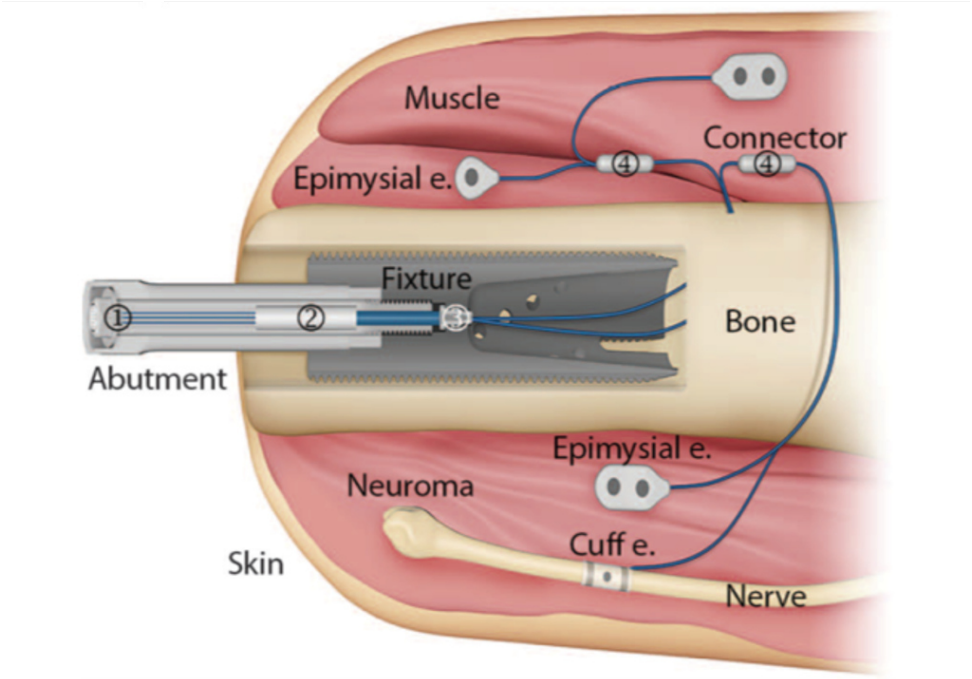

Figure 2: Schematic overview of e-OPRA Implant System. Image reference: [28].

1.2 Aim

This master thesis aiming to investigate the effect of electrical stimulation on osseointegration in titanium implants, with focus on the impact of different pulsed current parameters. The thesis consists of three components, a literature review, development of an *in vitro* model, and performance of an *in vitro* study. The purpose of the literature review was to gain knowledge in the field which could be used in the designing phase and in the selection of stimulation parameters. The *in vitro* study investigated the impact of pulsed electrical stimulation on enhancement of osseointegration and whether different parameters and various values of such parameters had a beneficial impact on the outcome.

1.3 Specification of Issue Under Investigation

The thesis examines two unanswered questions. Firstly, how has electrical stimulation been provided with the purpose to promote osseointegration in previous studies and which span of value for electrical stimulation parameters have been used? Secondly, does pulsed electrical stimulation have a beneficial effect of promoting osseointegration and if various parameter values impacts the outcome? The issues are clarified and approaches to solve the problems are explained in the following paragraphs.

- **Research in the literature field**
  Perform a meta-analysis in the research field where the approach to gain knowledge is to search for scientific articles where they have analysed the effect of electrical stimulation on osseointegration. Then investigate if there are similarities or patterns between studies with significant or non-significant results.
- **Developing an *in vitro* model**
  Develop an experimental setup that allows multiple testing of electrical stimulation via implant and electrodes. The approach is to obtain inspiration from previous *in vitro* models and from the design of the e-OPRA Implant System.
- **Performance of an *in vitro* study**
  Examine the electrical stimulation's impact on important components of the osseointegration process such as osteoblast attachment, proliferation, and collagen production. Furthermore, investigate if there is a significant difference between various values of the applied current amplitude and frequency on studied outcomes.

1.4 Limitations

The scope of the thesis covers investigations of pulsed electrical stimulation for promoting osseointegration, where the implant is used as the cathode. The study is focused on enhancing the biological bonding between the bone and implant surface, therefore further investigations in bone fracture healing and inhibition of bacteria attachment by electrical stimulation will not be covered in the thesis. The *in vitro* model and the experimental setup concentrate on testing the electrical stimulation, no further investigation in other

types of parameters were performed. Therefore, parameters such as type of metal, surface coating, surface pore size, etc. were characterised during the design phase and not changed during the performance of the *in vitro* study.

The electrical stimulation was restricted to parameters used in peripheral nerve stimulation. Therefore, only biphasic asymmetric balanced charged pulses were examined since that is known to be safe for the patient and the system [29]. The study only tested the impact of one electrical stimulation parameter at a time, hence no consideration was taken regarding interference between different parameters. The model was simplified such that homogeneous cell medium was used, and no considerations were taken regarding different conductivities in bone and muscles. Furthermore, the system only included one type of cells, the osteoblastic cell line MC3T3-E1, therefore interference between different cell types was not studied in this thesis.

2 Methodology

The method of the thesis is divided in three parts, one theoretical and two practical parts. The theoretical part included a literature review and the practical parts consisted of the development process and the performance of the *in vitro* study.

2.1 Literature Review

The theoretical part contains a literature review in the research field which was carried out by reading scientific articles. The articles were found in the databases PubMed, Google Scholar and Chalmers University of Technology Library with the keywords: osseointegration, electrical stimulation, direct current stimulation, titanium implants, bone formation, osteoblast proliferation and differentiation. The information in the articles was then compiled in a literature review document with focus on electrode configuration, delivery of current and stimulation treatment. The information was used to perform comparisons in order to find similarities or patterns between studies with significant or non-significant results.

2.2 Development of *In Vitro* Model

This section includes product requirements of the experimental setup, final design of the model, how cell culture conditions were managed, cleaning and sterilising of relevant components and lastly verification of some product requirements.

2.2.1 Requirements

The initial phase of the development process started with looking into articles that have performed *in vitro* setups and use their model for inspiration. The setup used in the experiments was influenced by [6], [13], [30] and by the design of the e-OPRA Implant System. The experimental setup had some requirements that needed to be fulfilled in order to be able to run the experiments. The setup is divided in four parts, the container, implant, electrodes, and stimulation where each part has its own requirements. In Table 1 the product requirements for each part are stated.

Table 1: Experimental setup requirements divided into four parts, namely; the container, implant, electrode and stimulation.

Container	The container should 1. be waterproof to prevent leakage 2. have dimensions that minimise the amount of cell culture medium 3. have components that allow the implant to stand up 4. have components that allow the implant and the electrodes to stay in the same position during stimulation, but makes it possible to remove afterwards
Implant	The implant should 5. be of the same material as the implant fixture in e-OPRA, Ti6Al4V 6. have a flat surface in order to simplify the evaluation 7. have clinically-relevant dimensions, length 40 mm 8. have a wire connected to be able to stimulate
Electrode	The electrode should 9. have at least two electrodes in the setup for the possibility to test different configurations 10. have similar dimensions as in the e-OPRA Implant System 11. have a wire connected to be able to stimulate
Stimulation	The stimulation should 12. be of current control, in order to make sure that the delivered current is of the same amount throughout the experiment 13. have a function generator that can produce an arbitrary waveform in order to create the pulse used in peripheral nerve stimulation

2.2.2 Cell Culture Conditions

Despite the requirements for the setup, the essential conditions needed to satisfy the cells had to be taken into consideration as well. The cells needed to be cultured at 37 °C, 5% CO_2 and in >95% humidity. Those conditions are obtained in an incubator, although it was not possible to use an incubator due to a lack of power outlet inside the incubator that was available in the laboratory facilities. The condition was instead obtained in a heat box to manage the temperature, and N-2-hydroxyethylpiperazine-N-ethanesulfonic acid (HEPES) buffer was added in the cell medium to obtain 5% CO_2. To avoid a large amount of evaporation a lid was used that covered the container in the heat box. Sterilised water was also added in plastic containers which were placed both inside and outside the lid.

2.2.3 Final Design

The final design of the experimental setup included a 3D-printed container made of polylactic acid (PLA), a plate and two discs made of Ti6Al4V, a bipolar constant current stimulator (DS5, Digitimer) and an Arbitrary Function Generator (AFG-2112 - 12MHz, Gwinstek).

The container is a rectangular box which was designed with several different features in order to fulfil the requirements. The device contains two different positioners, one for the implant and two for the electrodes. The implant positioner has two separated components that allows the implant to stand up by sliding into two slots. The slot nearest the wall was designed with an output that allowed the wire to exit the container. The electrode positioner contains a cylindrical extrusion with an opening closest to the wall in order to let the wire exit. The container has three rectangular slots in the upper part of the wall, two located at the long side and one positioned at the short side. Those slots were designed in order to prevent rotation and restrict movements of the implant and the electrodes during the experiment. Figure 3a visualises a CAD sketch of the box where the feature and the dimensions are pointed out, while Figure 3b shows a photograph of the experimental setup with the electrodes and implant put in place.

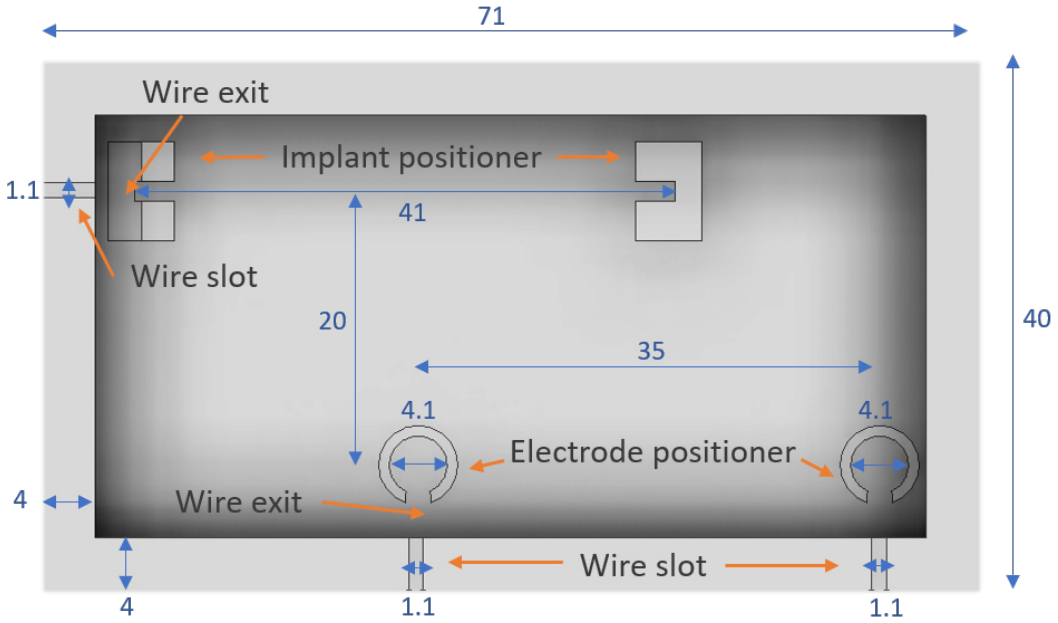

(a) CAD sketch

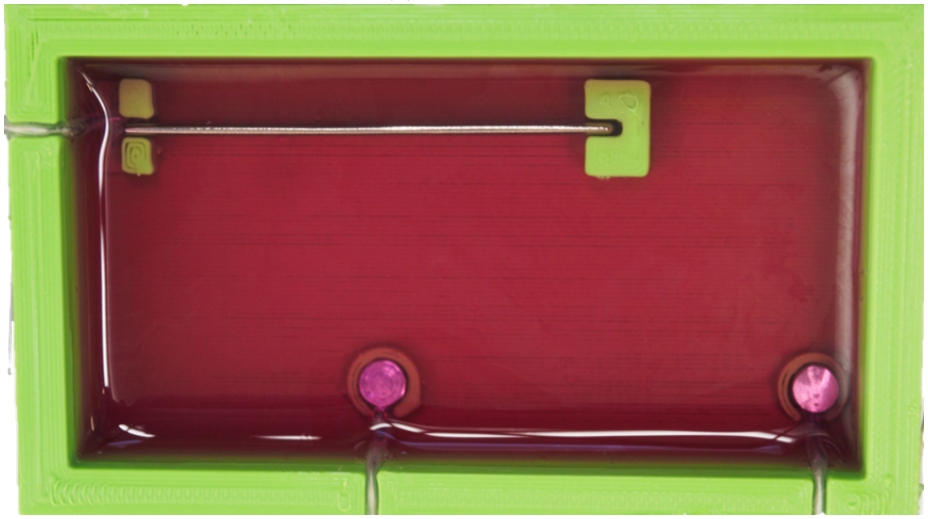

(b) Experimental setup

Figure 3: Experimental setup, where the CAD sketch in a) displays the features and the dimensions of the device and b) shows a photograph of the experimental setup.

The Ti6Al4V plate was chosen to imitate the implant fixture with the size of 40x4 mm and a thickness of 1 mm. The discs were chosen to act as electrodes with a diameter of 4 mm and a height of 3 mm. The wires that connected the plate and the discs to the current generator were made of titanium grade 1 (Sargenta AB) with a length of 10 mm where the part of the wire that was in the cell culture medium was isolated within a silicone tube. In order to prevent corrosion between the wire and the implant, and leakage due to the capillary effect in the silicone tube, a small droplet of silicone glue (Med-1037, Nusil) was used to cover the welding and prevent the media from being sucked out through the tube. The function generator was used to control the bipolar constant current generator that sent out the pulse with pre-programmed characteristics. The implant was connected to the negative output, working as a cathode and the electrodes were connected to the positive output working as anodes. In order to produce replicates with the same amount of applied current, several boxes were coupled in series where the implant in one container was connected to the electrodes in another container. Figure 4 visualises the circuit with one container.

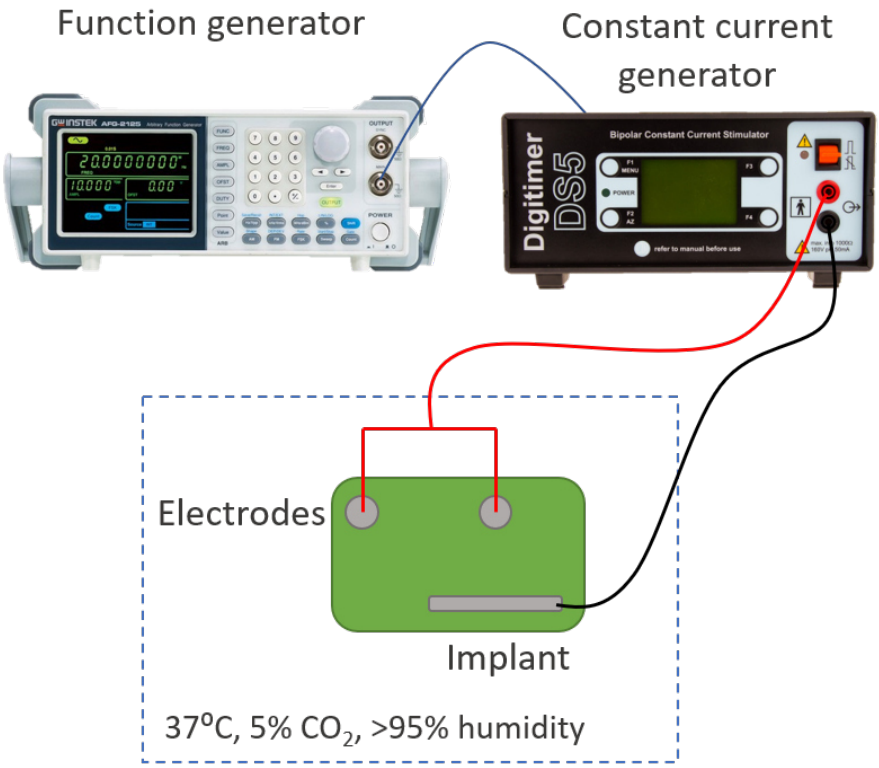

Figure 4: Schematic overview of the circuit in the experiment with one container.

2.2.4 Cleaning and Sterilisation

The implants and electrodes were rinsed to remove dust and oils by cleaning cycles with extran (MA 02, Merck) and deionized H_2O in an ultrasonic bath with the heat of 70 °C. They were sterilised in an autoclave for 20 min in 121 °C. For the sterilising protocol see Appendix A.1. The 3D printed containers were rinsed in cleaning cycles with extran (MA 02, Merck) and deionized H_2O in an ultrasonic bath with cold water following the protocol in Appendix A.2. They were sterilised under a UV lamp for 25 min. See Figure 5.

(a) Cleaning implants and electrodes **(b)** Cleaning containers.

Figure 5: Cleaning of experimental parts in the ultrasonic bath, a) implants and electrodes and b) containers.

2.2.5 Verification Testing of Experimental Setup

Some of the product requirements needed to be verified by performing tests. Firstly, the material of the implant needed to be characterised. This in order to confirm elemental composition, topography and investigate if there was contamination, dirt or bacteria, on the implant surface after cleaning and sterilisation. The container was tested for leakage and for evaporation. Lastly, the setup was tested for impedance measurements in order to calculate the correct applied current.

2.2.5.1 Characterisation of Implant Material

Characterisation of the implant surface was achieved by scanning electron microscopy (SEM) imaging, with accelerating voltage of 3 kV and working distance of 5 mm. Elemental composition of the implant material was confirmed by energy dispersive X-ray spectroscopy (EDX) with accelerating voltage of 20 kV and working distance of 10 mm.

2.2.5.2 Contamination Testing

Contamination testing was performed on the whole experimental setup with every part assembled and on a cleaned and sterilised implant separately. The testing of the whole setup was performed by using cleaned and sterilised parts, assembling them and filling the container with 12 ml cell culture media that was used during the experimental cycles, two replicates of the setup was used. Then the containers stayed for 3 days in the heat box. The implants where placed in Falcon tubes filled with bacteria growth medium, tryptic soy broth (TSB), with one control and the tubes stayed overnight in 37 °C. A cleaned and sterilised implant was analysed for bacteria and dirt contamination by performing SEM imaging with accelerating voltage of 3 kV and working distance of 5 mm.

2.2.5.3 Leakage Testing of Container

The container was tested for its waterproof property by filling the container with water after applying and letting the silicone glue dry for at least 1 h. If the container started to leak, a second layer of the glue was applied. The containers were then cleaned and sterilised by the procedure mention in previous paragraph. After experiencing that the cleaning cycle could in some way cause holes in the silicone layer that caused leakage, the containers were tested for leakage after cleaning and sterilisation inside a sterile fume hood with sterilised water before the experimental cycle started.

2.2.5.4 Evaporation and Temperature Testing

Results from preliminary testing displayed uneven evaporation in containers located at the back nearest the heat fan compared to the front closest to the opening of the heat box. The evaporation in the containers placed at the front even had that much evaporated cell culture media that the top of the implant surface was uncovered. Therefore, evaporation of cell culture medium was monitored during a period of 15 h in order to be able to predict how much medium that needed to be refilled every 24 h. Three containers were placed in the back and three were placed in the front, and a lid was placed over the containers with medium and containers with sterilised water were place inside and outside the lid. Five data points were noted at the time points 0, 1, 2, 3 and 15 h and the data that was collected was the temperature of the medium and the amount of medium left in the container.

2.2.5.5 Impedance Measurement

To be able to apply the right current the impedance in the cell culture media needed to be measured. The measurement was obtained by positioning the implant and the electrodes in the container, it was then filled with cell culture media and the impedance measured with a multimeter (UNI-T UT131B, Clas Ohlson), see Figure 6.

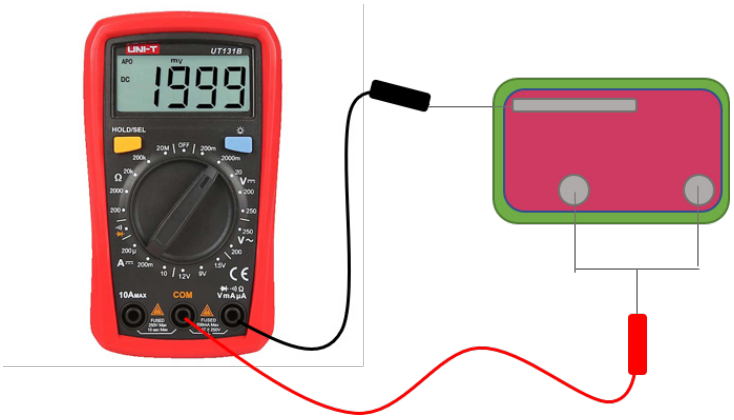

Figure 6: Schematic overview of the impedance measurement with a multimeter. Notice that the value showed in the multimeter display is not the measured value.

2.3 *In Vitro* Study

This section contains the performance of the designed *in vitro* model for testing the electrical parameters including cell culture, pulsed electrical stimulation and the stimulation treatment. It also includes the evaluation assays, which examine the cell proliferation, collagen production, cell distribution, cell morphology and attachment.

2.3.1 Cell Culture

The used cell line was the osteoblastic cell line MC3T3-E1, established form C57BL/6 mouse calvaria. The cells were cultured in Dulbecco's Modified Eagle's Medium (DMEM) containing 4.5 g/l D-glucose, L-glutamine and 25 mM HEPES, which was supplemented with 10 % fetal bovine serum (FBS) and 1 % penicillin-streptomycin, 0.25 mg/ml amphotericin-B. This solution will be referred to as supplemented DMEM (sDMEM). For the experiments, an osteogenic differentiation medium was used, where sDMEM was further supplemented with 1 % L-ascorbic acid 4.5 mM, 1 % dexamethasone 1 mM and 2 % β-glycerophosphate 1 M. The cells were cultured at standard conditions of 37°C, 5% CO_2 and >95% humidity. The cell line used in the experiments was of passage 10, and the same vial was used for all experiments.

The cells were precultured to the implant surface in a 2 ml Eppendorf tube, see Figure 7, for 16 h with a seeding density of 100 000 cells/implant. The implant surface facing the electrodes in the experimental setup was placed upwards, and a small piece of tape on the wire was used to restrict movements of the implant. Six random implants were counted directly after the preculturing before starting the experiment in order to have controls for how many cells attached to the surface. For the preculturing sDMEM was used and the implants were cultured in an incubator at standard cell conditions. After preculturing, the implant was transferred to the experimental setup and placed in its positioner. The electrodes were as well placed in their positioners and connected to the generators. 12 ml of osteogenic differentiation medium was added to the container and the experiment started when electrical stimulation was applied.

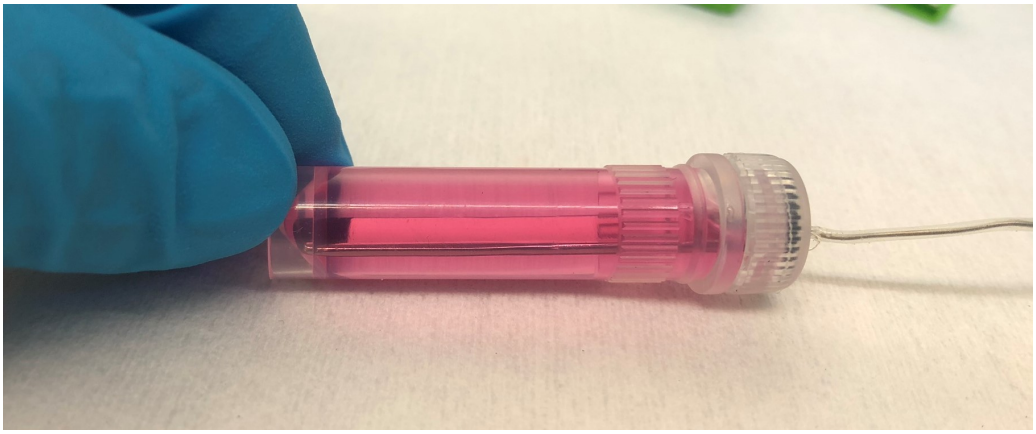

Figure 7: Preculturing of an implant in an Eppendorf tube, where the wire goes out through the lid via a custom made hole and the total amount of cells in the sDMEM is 100 000.

2.3.2 Pulsed Electrical Stimulation

The electrical stimulation consisted of pulses with similar properties that are used during peripheral nerve stimulation to restore sensory feedback. The same pulse was chosen since it is clinically proven that this pulse is harmless for the patient and the electrical control system [27]. The pulse is charge-balanced, cathodic, rectangular, biphasic asymmetric (10:1) and current-controlled, see Figure 8. The cathodic phase (negative pulse) is followed by an inter-pulse break (zero amplitude) and then by a recovery phase (positive pulse). The recovery pulse shall have an amplitude 10 times smaller and a duration 10 times longer than the cathodic phase. Each stimulation pulse is followed by a charge recovery phase where any residual charge is recovered back to zero to ensure that charge accumulation cannot occur.

Figure 8: The peripheral nerve stimulation pulses are charge-balanced, cathodic, rectangular, biphasic asymmetric (10:1), and current-controlled. The illustration indicates negative amplitude (NA), positive amplitude (PA), negative pulse width (NPW), inter pulse break (IP), positive pulse width (PPW) and charge recovery (CR).

2.3.3 Stimulation Treatment

The study consisted of 5 different groups where various conditions were applied: 1 control group and 4 groups which received stimulation, with 5 replicates in each group, see Table 2. Two parameters were investigated, negative pulse amplitude and frequency, where one of the parameters were tested at the same time and the other parameters were then set to a fixed value. In the groups, A10F50, A20F50 and A50F50, an amplitude screening was performed with amplitudes of 10, 20 and 50 μA. In A20F100 the frequency value was increased from 50 Hz to 100 Hz and in the control group no stimulation was applied. Every cycle of experiment was running for 72 h with continuous pulse stimulation, with a short break of 10 minutes every 24 hours when media refill was performed. The fixed parameters of the pulse were: negative pulse width (NPW) which was set to 500 µs, the inter-pulse break which was set to 50 µs and sample frequency fixed to 100 kSPS. In each stimulated group, three replicates was evaluated for cell count and two replicates was prepared for SEM imaging. Every replicate was evaluated for collagen production.

Table 2: Stimulation treatment for control, A10F50, A20F50, A50F50 and A20F100.

Group	Replicate	Amplitude (μA)	Frequency (Hz)
Control	1	-	-
	2		
	3		
	4		
	5		
A10F50	6	10	50
	7		
	8		
	9		
	10		
A20F50	11	20	50
	12		
	13		
	14		
	15		
A50F50	16	50	50
	17		
	18		
	19		
	20		
A20F100	21	20	100
	22		
	23		
	24		
	25		

2.3.4 Evaluation Assays

This section includes the different evaluation assays that was performed, consisting of cell count, collagen production and SEM imaging.

2.3.4.1 Cell Proliferation

To measure the number of attached osteoblasts to the implant, a NucleoCounter was used. Three replicates in each stimulation group were counted for attached cells. The implant was first removed from the container into a 2 ml Eppendorf tube then the cells were detached with 200 µl lysis buffer (Reagent A100, Chemometec). The tubes were vortexed for 30 s and 200 µl of stabilisation buffer (Reagent B, Chemometec) was added and the tubes were vortexed for 30 s once again. The liquid was taken up in a NucleoCounter cassette and the total number of cells was counted with the machine. The NucleoCounter presents the result as number of cells per ml, therefore the given number was multiplied with a factor of 0.4 since 400 µl was added in total to the Eppendorf tube.

The NucleoCounter software view provides a visualisation of each sample, where it presents a fluorescence image which allows for further validation of the cell count and higher accurate estimation of values that was below detection limit, <5000 cells/ml. The replicates with a cell count above detection limit were used in order to find a relationship between pixel coverage and number of cells. The images were analysed in the software Fiji ImageJ where histogram and a noise threshold for each image were provided. In order to take the intensity into consideration as well as the pixel coverage, the number of the grey scale was weighted with the number of pixels by performing a multiplication of the two values. The sum of the weighted values was then normalised against a fully white image, which presents the coverage percentage. The percentages for each sample were plotted against the numbers that the NucleoCounter provided in order to analyse the cell count and estimate the values below detection limit.

2.3.4.2 Production of Collagen

To measure the amount of soluble collagen in the cell culture medium after the experimental cycle a collagen kit was used, (Sircol Soluble Collagen Assay, Biocolor). The medium for every replicate in each experimental group was collected and diluted to 11.5 ml in order to take uneven evaporation into consideration. The samples were prepared according to the protocol in the kit, see Appendix A.3, and absorbance measurements was performed at 555 nm by a microplate reader (FLUOstar Omega, Bmg Labtech).

2.3.4.3 Cell Distribution, Morphology and Attachment

To analyse the distribution, morphology, and attachment of cells on the titanium implant SEM imaging was applied to visualise samples under high magnification. SEM was used as a qualitative evaluation, where two implants in every stimulated group were prepared for SEM imaging. The control group was not SEM imaged, due to limited number of implants. In brief, the samples were fixed in 4 % paraformaldehyde for 2 h at room temperature and stained with 1 % osmium tetroxide for 2 h. After another rinse with buffer, the samples were briefly dehydrated in a graded ethanol series for 5 min per cycle (50, 70, 80, 90, 95 and 100 % ethanol) and allowed to dry in air. The samples were sputter-coated with gold before examination in an Ultra 55 FEG SEM (Leo Electron Microscopy Ltd, UK) with settings of 5 kV accelerating voltage, 5 mm working distance and 30 μm aperture size.

2.3.5 Statistical Analysis

The data was statistically analysed using an unpaired, two-sided, homeostatic t-test at a significance level of 5% ($p < 0.05$).

3 Results

This section contains the results from the literature review, the development process of the *in vitro* model and lastly results from the evaluation assays in the *in vitro* study.

3.1 Literature Review

The results from the literature review are compiled in an article draft that is found in Appendix C. The article is submitted to the *Journal of Neuroengineering and Rehabilitation*.

3.2 Development of *In Vitro* Model

In this section results from the verification of the *in vitro* model is presented, including characterisation of implant material, contamination testing, leakage testing of container, impedance measurement and lastly evaporation and temperature testing.

3.2.1 Characterisation of Implant Material

The surface of the implant had common features that are often found on a machined implant surface. Figure 9 displays a SEM image in 2D of the implant surface, where the arrows in the image points at features discovered on the implant surface. The groves and flakes, 1 and 2, are found throughout the whole surface in an irregular pattern with different shapes, dimensions, and depths. The black dots pointed out by arrow number 3 shows that despite the cleaning there is still some dirt left on the surface.

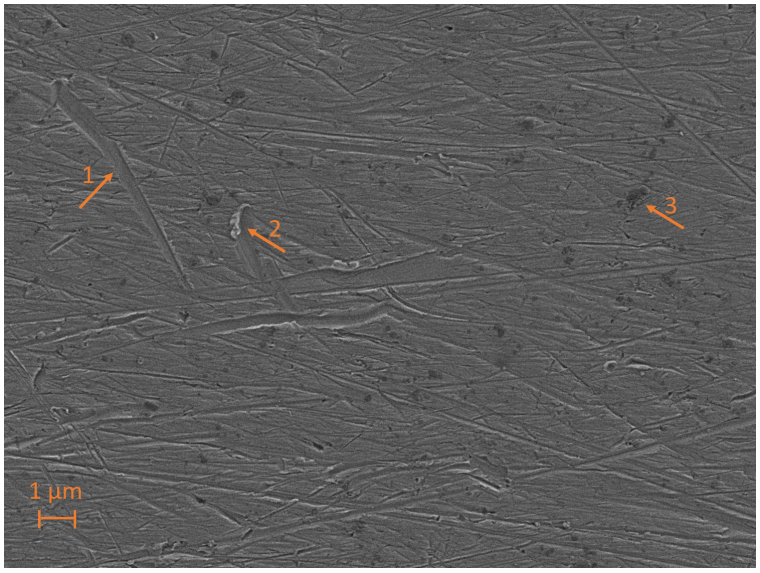

Figure 9: SEM image of a cleaned and sterilised implant surface. The arrows point out commonly found features on a machined implant surface, 1 grooves, 2 flakes and 3 carbon contamination.

The K_α values for the elements in the alloy Ti6Al4V are 4.5, 1.48 and 4.9 KeV for titanium, aluminium and vanadium respectively [31]. The L_α value for titanium is 0.45 KeV [31]. At those KeV values there should be a peak if the elements are found at the implant surface. The EDX spectrum in Figure 10 reveals four peaks at 0.48, 1.495, 4.5 and 4.92 KeV where the intensity is higher. All peaks represent one element in the alloy.

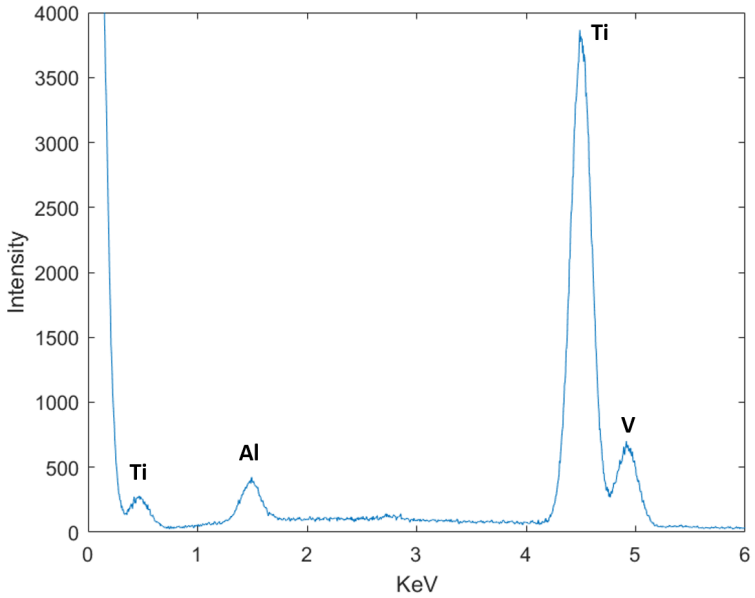

Figure 10: Energy dispersive X-ray spectrum of the implant surface, where intensity is plotted against KeV. The spectrum has peaks at 0.48, 1.495, 4.5 and 4.92 KeV.

3.2.2 Contamination Testing

When observing the bacteria growth medium there was no visible bacterial growth in the Falcon tubes. The growth medium in the replicates had the same transparent colour as the reference tube. If there was any bacteria contamination in the experimental setup with every part assembled the growth medium should have been less transparent and more turbid compared to the reference tube. The cleaned and sterilised implant had no bacterial contamination as well as the setup, however carbon contamination was visible during the surface characterisation.

3.2.3 Leakage Testing of Container

The 3D printed structure was not waterproof by itself, it started to leak a few minutes after adding liquid to the container. Therefore, silicone glue (MED-1037, Nusil) was applied, and the liquid then stayed nicely in the container. Due to the uneven surface of the 3D structure, it was hard to apply an even layer of the silicone glue which in some cases lead to pores in the layer where liquid leaked out. Those pores were more frequently located at the corners of the container. This led to application of several layers of glue and several tests of leakage before and after cleaning and sterilisation. The tests after sterilisation was performed in a sterile fume hood with sterilised water.

3.2.4 Evaporation and Temperature Testing

The vaporised cell culture medium in containers placed at the back versus front is displayed in Figure 11a as well as the temperature in Figure 11b. The data is presented as the mean value of the three containers back and front at every time point. The trendlines are plotted as exponential functions. When looking at the data for the containers placed at the back, blue, all data points lie above the critical line, where the critical line indicates the amount of cell culture medium that is needed to cover the whole implant surface. The trendline at 24 h does not cross the critical line as well, implying full coverage of the implant surface in the containers placed at the back after. The data points for the containers located at the front, green, has a similar trend as the blue data points at t=1, 2, 3 h, but the negative gradient is larger. The green data point at 15 h is already below the critical line, as well as the value of the trendline after 24 h. The data indicates that the implants placed at the front, will have a portion of the implant surface that stands above the cell culture media.

Figure 11b visualises the temperature in the cell culture medium in the containers placed at the back, blue, and at the front, green. The cell culture medium in all containers have the same temperature at t=0. After 1 h there is a difference of 3 °C between the containers back and front. At 3 h the medium temperature reaches the temperature of the heat box, 37 °C, and there is a difference of 0.8 °C in the boxes front versus back. After 15 h there is still a difference, but it has decreased to 0.4 °C.

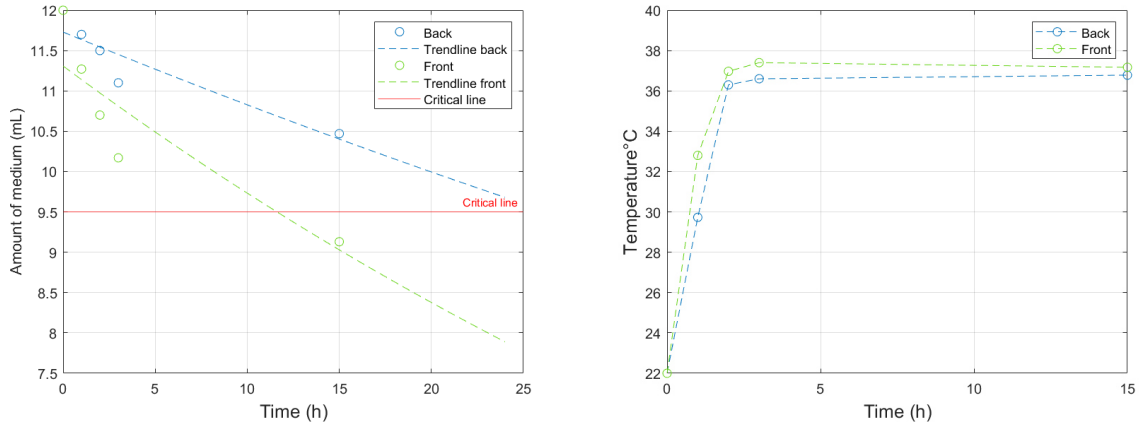

(a) Evaporation of liquid

(b) Temperature

Figure 11: Evaporation of cell culture media in containers placed back, blue, vs front, green, in the heat box in a) where the critical line indicates the level of the cell culture medium that is needed to cover the whole implant surface. In b) the temperature at different time points for back, blue, and front, green.

3.2.5 Impedance Measurement

The impedance of the cell culture medium between the implant and electrodes was measured to be 500 kΩ. This value was taken into consideration when calculations were made to obtain the right amount of applied current during the stimulations.

3.3 *In Vitro* Study

This section provides the results from the *in vitro* study, including data for cell proliferation, collagen production and SEM images for cell distribution, morphology and attachment.

3.3.1 Cell Proliferation

Figure 12 displays two visualisations that the NucleoCounter provided for each replicate, to the left, a replicate with low cell count and to the right, a replicate with high cell count number. In Appendix B.2 the fluorescent images for each replicate can be found.

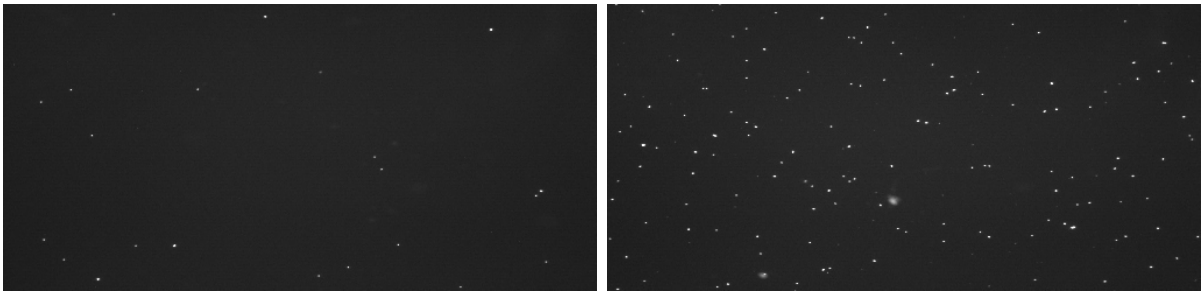

(a) Control, replicate 4, 4000 cells **(b)** A20F100, replicate 22, 28800 cells

Figure 12: The fluorescent images provided by the NucleoCounter. In a) a replicate from the control group with a cell count of 4000 cells and in b) from a replicate in A20F100 with a cell count of 28800 cells.

Two replicates, 1 and 3, in the control group received a cell count below detection limit, <5000 cells/ml, from the NucleoCounter. To obtain more correct values for these replicates, the area coverage for each sample was calculated and plotted against the cell count provided by the NucleoCounter. The linear regression has a function of $y = 1.0002E^{-5x} + 0.006176$, $R^2 = 0.9296$ and is statistically significant, $p = 7.24E^{-9}$. The function provides cell count values of 500 for replicate 1 and 1900 for replicate 3. The data for the area coverage is found in Appendix B.3 and the plot is found in Figure 26 in Appendix B.2.

The cell proliferation is presented in a boxplot, see Figure 13, where each box represents one group. In the stimulated groups there are three replicates per group and in the control group there are five replicates. The data for each replicate is normalised against the mean value of the counted number of cells after preculturing, 24600. Data for preculturing is found in Appendix B.1 and cell proliferation data after 72 h for each group is found in Appendix B.3. The y-axis in Figure 13 indicates the cell proliferation, where 1 is straight after preculturing, at time point 0 h. The control, A10F50, A20F50 and A50F50 have mean values below 1, meaning that the cell population on the implant surface has decreased from time point 0 h to 72 h. The cell proliferation decrease is greatest in the control group, and the decrease in A10F50, A20F50 and A50F50 is significantly smaller compared to the control group. (A10F50: $p = 0.022$, A20F50: $p = 0.00036$, A50F50: $p = 0.00053$). There is no significant difference between the amplitude groups, A10F50,

A20F50 and A50F50, but the mean value for A20F50 is higher than both A10F50 and A50F50. A20F100 is the only group where the cell population has increased during the period of 0 h to 72 h. The cell proliferation in the group is significantly higher compared to the control, $p = 1.617E^{-6}$, and compared to A20F50, $p = 0.0199$.

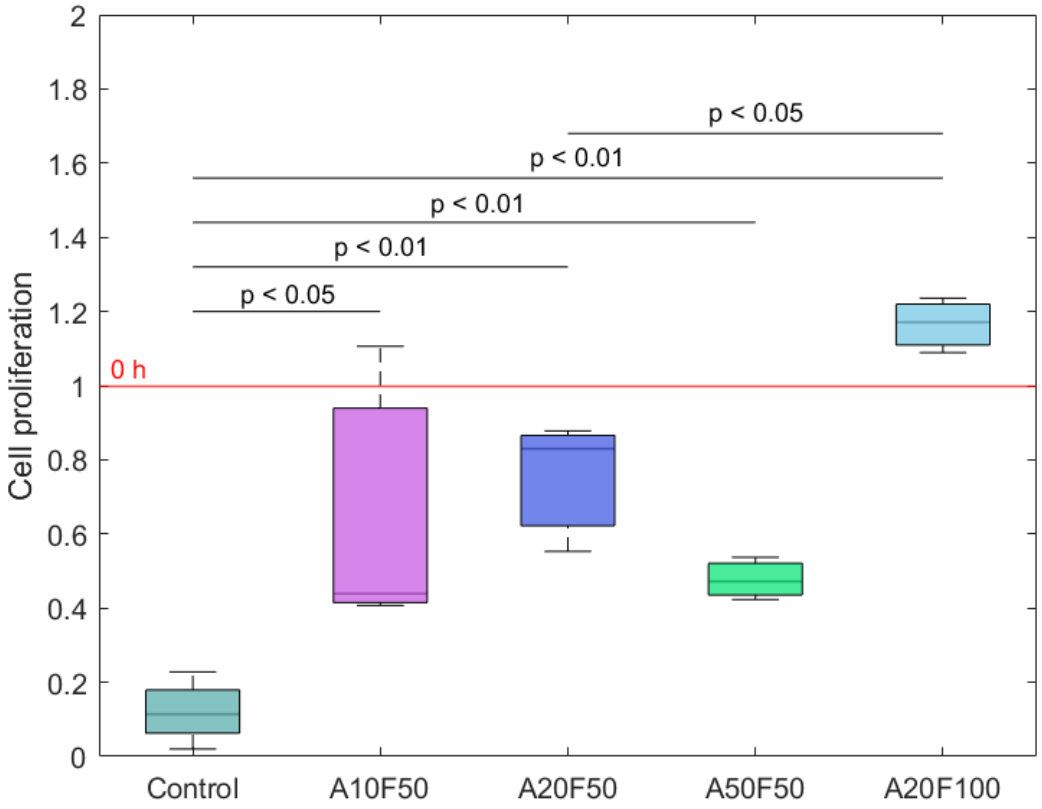

Figure 13: Cell proliferation of each group, where the data is presented as the normalised values against the mean of the preculture, 24600. In the control group n=5 and in the stimulated groups n=3. 1 at the y-axis implies the amount of cells at time point 0 h.

3.3.2 Production of Collagen

The collagen production for each group is presented in a boxplot in Figure 14, where there are five replicates in each group. The data was obtained in values of OD_{555nm} and transformed to values of μg collagen by the standard curve function $y = 5.1528 * x$, $R^2 = 0.9665$. To receive a more accurate value of every replicate, three technical replicates of each sample were measured. Each replicate is presented as the mean value from the 3 technical replicates. The raw data for the collagen production is found in Appendix B.4.

When looking at the amplitude screening there is a significant difference between A10F50 and A20F50, $p = 0.039$, and between A10F50 and A50F50, $p = 0.0078$. The collagen production in both A20F50 and A50F50 is significantly higher compared to the control group, $p = 0.033$, $p = 0.011$, respectively. A20F100 has a significantly higher collagen production compared to the control, $p = 0.00053$ and compared to A20F50, $p = 0.0094$.

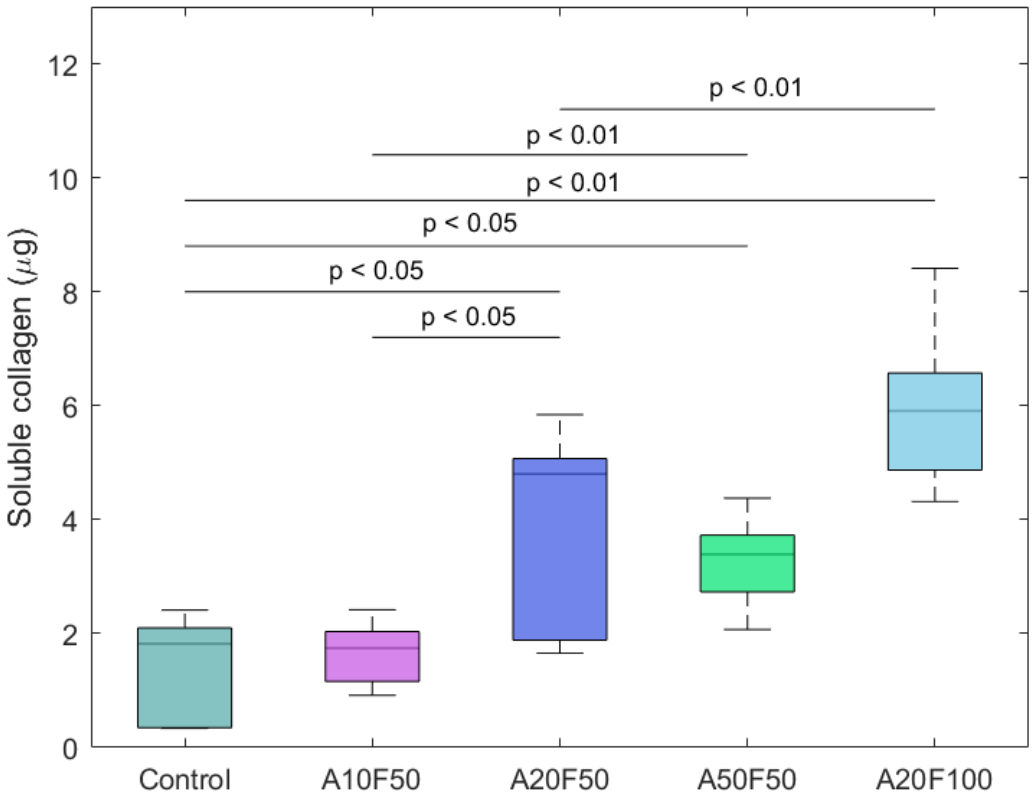

Figure 14: Collagen production presented in μg for each group, where n=5 in every group.

3.3.3 Cell Distribution, Morphology and Attachment

The section is divided in two paragraphs, where the first paragraph visualises SEM images with low magnification in order to provide the distribution of cells throughout the implant. The second paragraph includes SEM images with high magnification to show cell morphology and attachment of the cells in the different groups.

3.3.3.1 Distribution

The cell distribution on the implant surface in the different groups are displayed in Figure 15. The SEM images representing the cell density throughout the implant where the images to the left in Figure 15 are located nearest the wire and the images to the right display the cell density furthest away from the wire. The images in the middle represent the part in between, notice that those images can differ in location between the different groups. The dark spots in the images represent the cells, whereas the lighter background presents the implant surface.

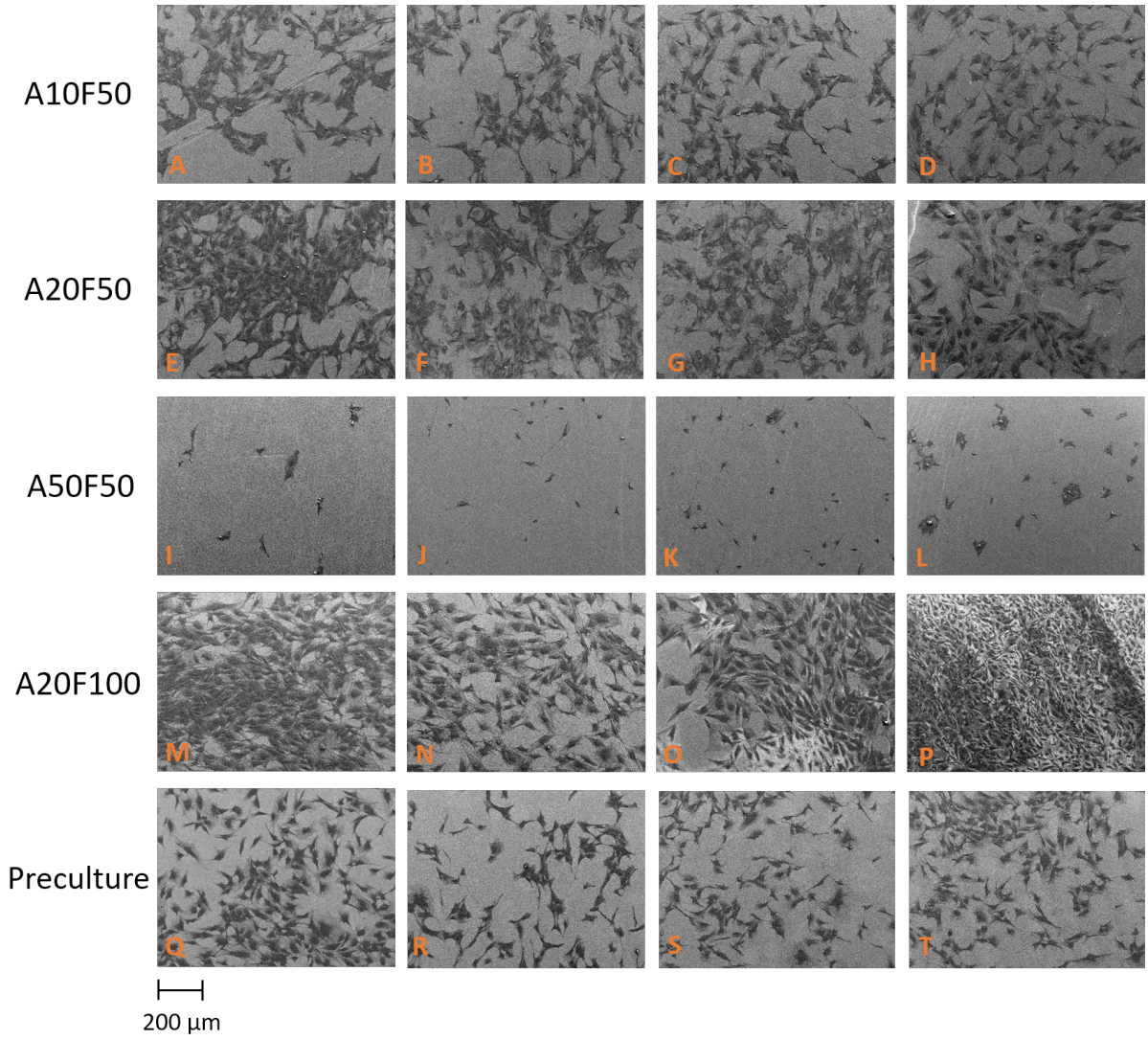

Figure 15: Cell distribution presented by SEM images throughout the implant. The images are sorted, where the part closest to the wire is presented in the images to the left and the part furthest away to the right in the figure. The images in between represent the middle part of the implant, notice that those images are not taken in the exact same position in every group. a)-d) A10F50, e)-h) A20F50, i)-l) A50F50, m)-p) A20F100 and q)-t) preculture.

3.3.3.2 Cell Morphology and Attachment

The cell morphology and cellular attachment to the implant surface are presented for the different groups in Figures 16 to 20. Each group includes SEM images with magnification between 200x and 25000x. The images for each group are selected in order to present the characteristics for the group. The stimulated groups A10F50, A20F50, A50F50 and A20F100 have matrix structures (represented in the Figures 16 to 19 c and d), where those structures have the highest density in the A20F50 group. The matrix structures are not visible in the preculture, although the preculture group have thread like structures on the surface, which are not showed in the stimulated groups.

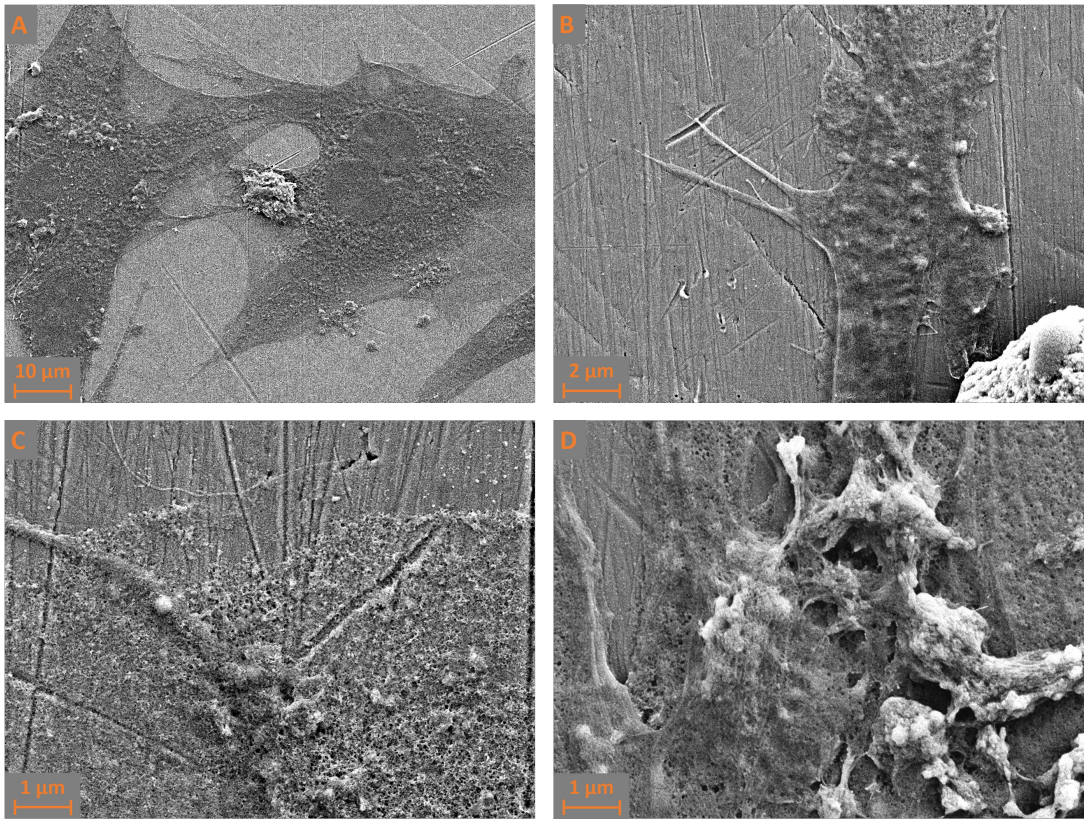

Figure 16: SEM images a)-d) presenting group A10F50.

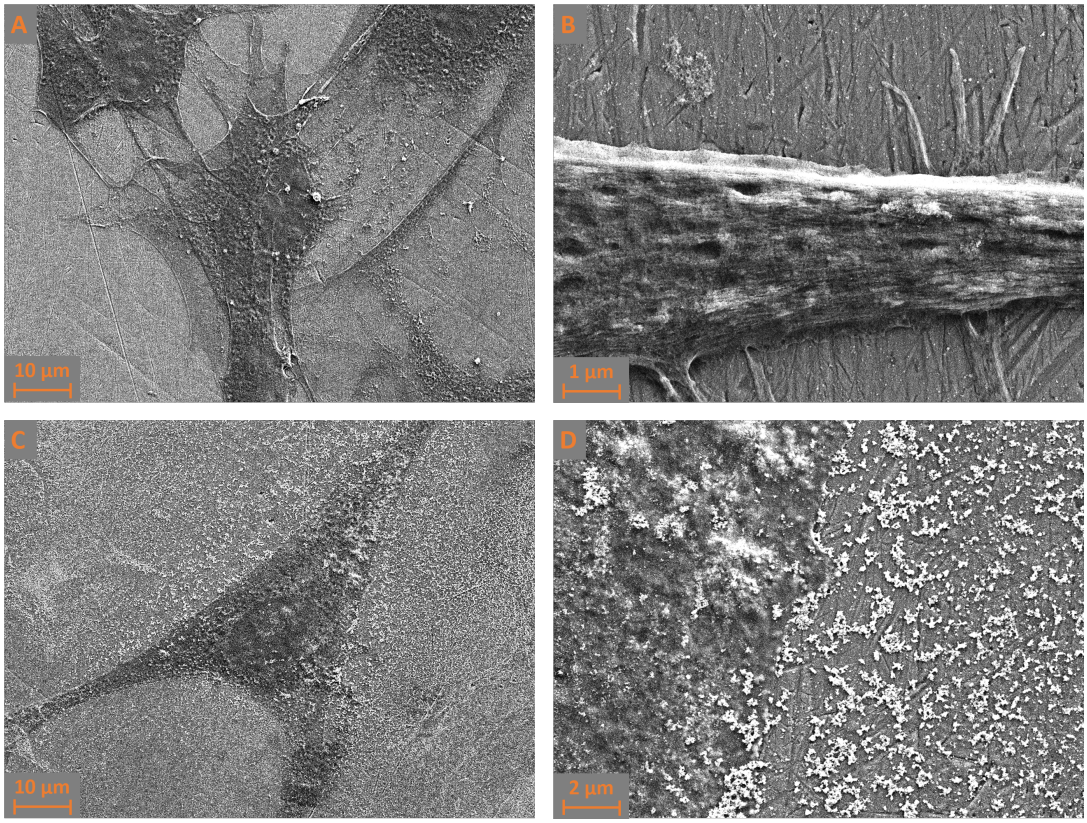

Figure 17: SEM images a)-d) presenting group A20F50.

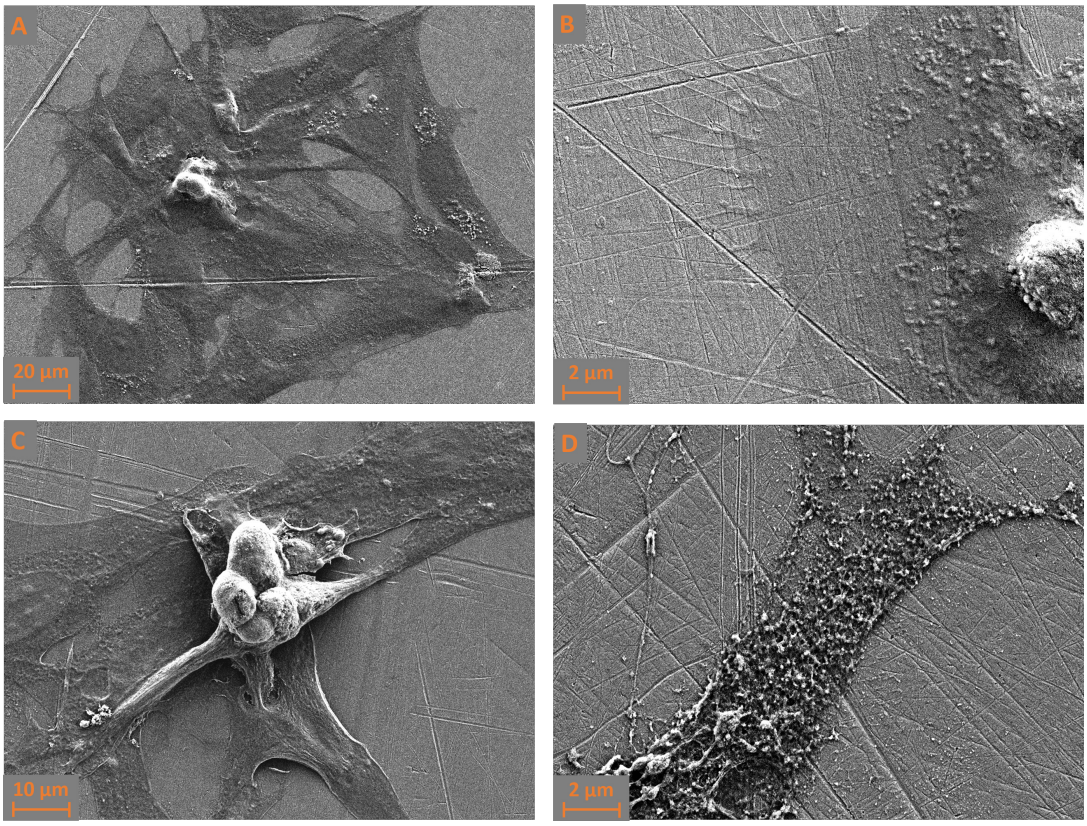

Figure 18: SEM images a)-d) presenting group A50F50.

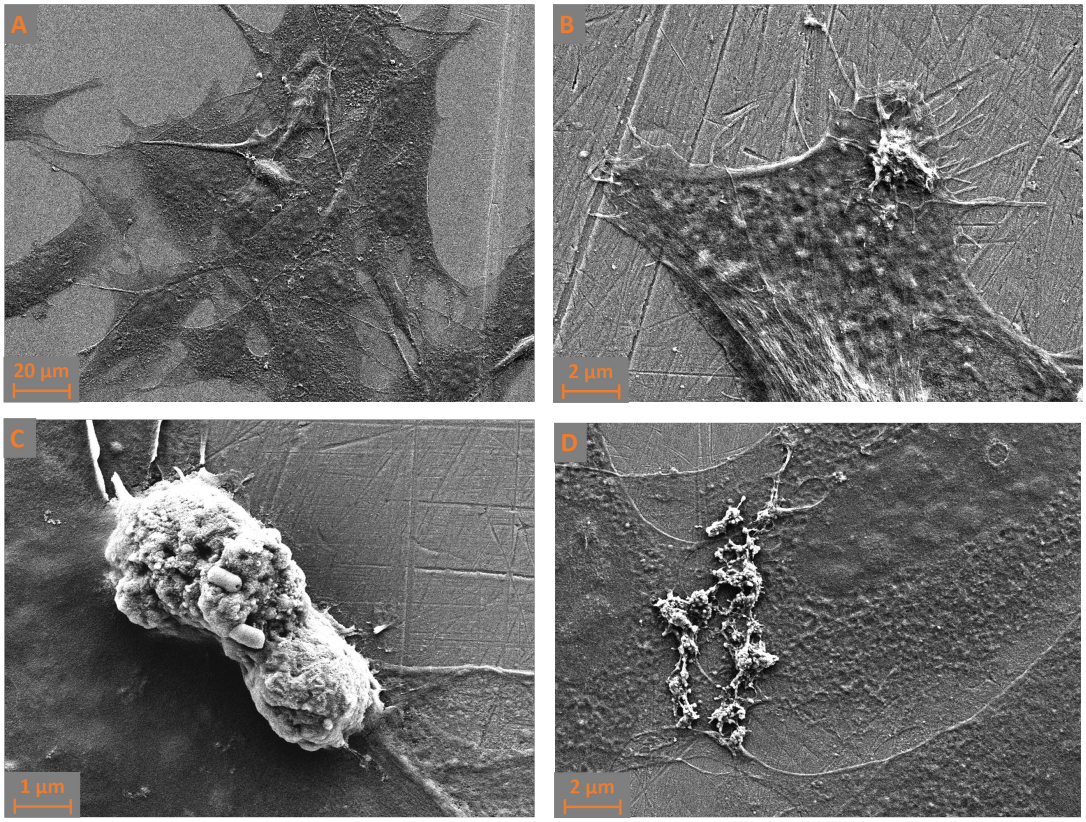

Figure 19: SEM images a)-d) presenting group A20F100.

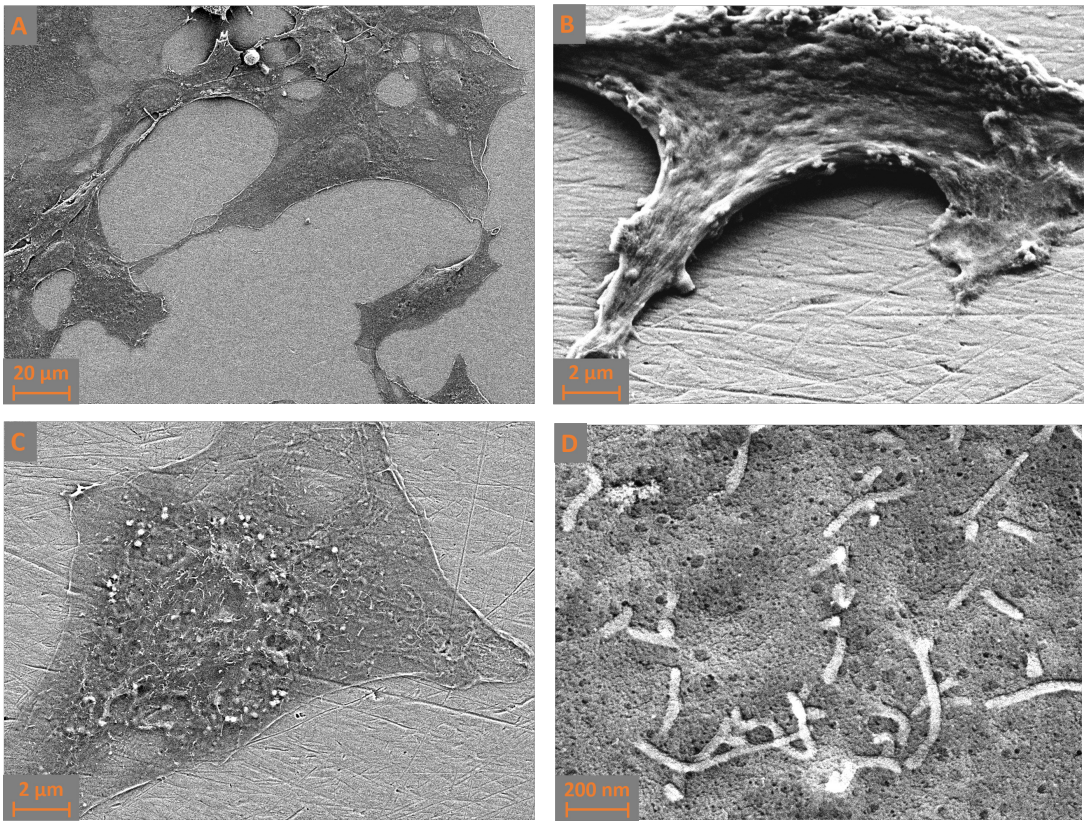

Figure 20: SEM images a)-d) presenting the preculturing group.

4 Discussion

The discussion is divided between the *in vitro* model, the evaluation assays and the pulsed electrical stimulation.

4.1 *In Vitro* Model

This section includes obstacles that was faced during the development process and during the *in vitro* study. Furthermore, it includes limitations with the model and further development potentials.

4.1.1 Obstacles Faced During the Development Process and *In Vitro* Study

The first choice faced during the development process was the choice of which type of container that should be used. The implant dimension reduced the number of container alternatives. A regular 6-well plate was too small to fit the configuration of implant and electrodes that was wanted, and a larger petri dish had too much dead space in the areas above and below the implant and electrodes. The dead space required a larger amount of medium, which did not fulfil product requirement number 2 in Table 1. Another problem that needed to be solved if using a well plate or petri dishes concerned components that restricted movements of the implant and electrodes during stimulation. An alternative that was considered was to glue the implant and electrodes at their positions with biocompatible silicone glue. This solution would have reduced the option of easy removal, and adding another substance to the cell environment would have increased the number of factors that can potentially have an impact on the outcome. Therefore, a 3D printed structure was considered since it enabled a custom-made design that could minimise the dead space and meet the other product requirements for the container.

Leaking containers was an unpredictable outcome during the test cycles, even if the containers had been tested before starting the experimental cycle. In one case the container was waterproof for 2 days and started to leak at day 3, which caused loss of a valid data point and of course time. Several leakage situations resulted in more silicone glue layers and in an extra leakage test after the cleaning and sterilisation procedure. Since the cell culture medium included phenol red, tracking of where the leakage had arisen was in most cases easy. Small holes in the silicone glue layer could in most cases be found, and they were often placed at one of the corners of the container.

Uneven evaporation of cell culture medium in containers placed at the back of the heat box compared to the front, resulted in implant surface above the medium in the containers located at the front, as visualised in Figure 11a. If the implant surface is not covered in cell culture medium, the cells will dry out and die. If this scenario occurs at day 1, it will have a larger impact of the cell culture population compared to non-coverage at day 3. Comparison of containers placed at the back versus front was considered as invalid since the cells had not received the same conditions. Therefore, data points from implants placed in the front containers were excluded from the analyses. However, containers

placed at the back where electrical stimulation was applied had significant higher numbers, $p = 0.019$, of cells compared to the control that was standing side by side with the stimulated container. These results were collected during prestudies.

The uneven evaporation can be explained by the higher temperature in the containers placed at the front compared to the back, as seen in Figure 11b. More evaporation leads to a lower amount of media in the container and uncovered implant as mentioned before. However, when the medium vaporises it is only the water that goes away which means that concentration of waste products in the containers increases with higher evaporation. This creates a less favourable environment for the cells, and this in combination with uncovered implants can be some of the factors that caused the lower amount of cells attached to the implant in the containers located at the front.

In one of the last groups, A50F50, bacterial contamination was discovered in one of the replicates that was evaluated by SEM imaging. This replicate was considered to be invalid. There were no visible signs of bacteria in the other replicate that was evaluated by SEM imaging and the replicates that were counted in the NucleoCounter had a uniform number of cells. If the other replicates would have been contaminated, the environment in the container would have been unfavourable for the cells which would have led to reduced cell count. The pixels with higher intensity at the fluorescent images provided by the NuceloCounter present the nucleus from the cells. Since bacteria is a prokaryotic cell type, they do not have any nucleus, hence the pixels present nucleus from the cells and not from the bacteria. The cell medium in the replicates was still of a pink colour, indicating no pH change. Bacteria secretion often contains organic acids [32], and if bacteria contamination would have been the case the phenol red should have changed the medium colour to a more light yellow liquid. Therefore, the whole group was not excuded from analyses, only the replicate where bacterial contamination was discovered.

4.1.2 Limitations

There are limitations with the model that are important to highlight. Firstly, the model includes only one type of cell, the MC3T3-E1, and it does not consider how other cell types in the adjacent environment in an *in vivo* setting such as muscle cells, fat cells, macrophages etc. may be affected by the electrical field. The unicellular culture also reduces the signal pathways and interactions between different cell types which diminish the model from a real setting. MCT3T-E1 cells are isolated from mouse calvaria, resulting in possibilities of interspecies differences which need to be considered when transferring the results to further investigations. The cell line has a phenotypic differentiation from preosteoblasts to mature osteoblasts, but there have been signs of cellular replicative senescence in this cell line in high passages, $> p36$ [33]. However, the passage of the cell line used in the experiments was passage 10, which is a low passage, but it is important to keep this in mind.

The model is restricted to 2D, considering both the electrical field and the cellular network on the implant surface. In the human body, cells are spread out and interact with the environment in all three directions and a 2D cell culture is not a proper representative compared to a real cell environment. However, 2D cultures are well studied, there are lots

of comparative literature and they can work as an initial study. Another simplification of the model is the homogeneous environment in the cell culture media around the implant surface. In an *in vivo* model, various types of cells and tissues are organised between the bone anchored implant and the electrodes that are placed in the muscle tissue. This creates a heterogeneous environment where the conductivity in, e.g., cortical bone versus the muscle tissue differs resulting in effects on the electrical field.

4.1.3 Further Development

The model has the ability to be further developed in order to face the current limitations. A collagen matrix with immobilised cells could be a solution to several limitations with the model. The matrix opens up the opportunity for a 3D network of cells around the implant, where several cell types can be incorporated allowing for cell spreading in x, y and z-axis and allowing for signalling between cell types. A 3D matrix would provide a more accurate model of a tissue, hence results from a 3D model would provide results which are more similar to a real case scenario. However, a 3D scaffold around the implant makes the evaluation more complicated, where cell counting and measurement of collagen in the media will no longer be possible to perform.

4.2 Evaluation Assays

Three different evaluation assays were performed in the *in vitro* study, investigation of cell number, cell activity and cell morphology. In the cell proliferation assay, 2 out of 25 replicates were below detection limit in the NucleoCounter which resulted in calculated cell numbers for those replicates. The $R^2 = 0.9296$ value for the linear regression presented in Figure 26 is acceptable, but still low. Although, the calculated numbers provide a more equitable presentation than assuming the best case, 4999 cells/ml which results in 1999 cells/0.4 ml. The low R^2 for the linear regression can be explained by assumptions during the image analysis, too few data points or that the Nucleoview does not provide the whole image. Another reason for the low R^2 value can be that the NuceloCounter did not operate in its optimal range, since other values were also below or in the lower range of the optimal cell count for the NucleoCounter which lies in a range of $5x10^4$ to $5x10^6$ cells/ml [34].

In the evaluation for collagen production, a small amount of liquid, 100 μl was evaluated from the collected medium which was diluted to 11.5 ml. Uneven mix of the medium can cause difference in the collagen concentration in the sample. This factor was taken into consideration when producing three technical replicates of each sample to obtain a more accurate value. However, when looking at the raw data for the collagen production, many replicates have standard deviations of more than 50 % of the mean μg value, meaning that the collected data is well spread out, even if the technical replicate is collected from the same sample. Therefore, the collagen production evaluation can have misleading replicates. To solve this problem, more technical replicates could have been collected and evaluated.

Further evaluations that can be performed are measuring levels of bone formation hormones and growth factors to analyse cell activity and investigate the pathway of the enhanced proliferation and collagen production. Hormones and growth factors such as ALP can be analysed by performing RT-PCR and evaluate mRNA expression for the transcriptional expression of osteogenesis-related genes. This kind of evaluation would be another way to be able to further confirm higher cellular activity in stimulated groups compared to non-stimulated.

4.3 Pulsed Electrical Stimulation

When looking at the result for the cell proliferation in Figure 13, the population of cells have decreased in group A10F50, A20F50, A50F50 and the control compared to time point 0 h. However, the decrease in number of cells is significantly less in the stimulated groups compared to the control. The decrease of cells can have been caused by several factors. There is no guarantee that all cells that have attached during the preculturing will survive, some of them might already be preapototic. After 16 h, cells can have been attached, but in a poor way and mechanical forces during the transfer from the preculturing tube to the container can have physically caused removal of cells from the implant, where only cells that have attached strongly remains and poor ones are lost. During the verification testing, carbon contamination was visible throughout the implant even after cleaning, see Figure 9. This type of contamination impacts the surface tension, to which the cells are sensitive. Hence, it could be another factor involved in the decrease in population.

The interesting part to look at is the significant difference in cell survival between the stimulated groups compared to the control, where they survive poorly in the control and they survive significantly better in the stimulated specimens. Despite the decrease of cells, the number of survived cells on the stimulated surface was around 10 000 cells/cm^2, which is an acceptable number. The mean value in the A20F50 group is larger compared to A10F50 and A50F50, although there is no significant difference between the groups with different amplitude values. When comparing the two different frequencies, 50 and 100 Hz, there is a significant difference in the cell population and the A20F100 group is the only group where the population had increased in number compared to time point 0 h. Applying higher frequency for the pulses means that the time period between each pulse event decreases, and the more the stimulation resembles direct current.

The groups follow similar trends in the boxplots for cell proliferation and collagen production, which indicates that higher number of cells also results in higher production of collagen. However, there are some differences between them as well. The group where amplitude 10 μA was applied, A10F50, is not significantly higher in the collagen production compared to the control group. There is also a significant difference between the amplitudes which was not the case in the cell proliferation, where both A20F50 and A50F50 have a significantly higher collagen production compared to A10F50. The collagen production is as well significantly larger in A20F100 compared to A20F50 and the control, which follow the cell proliferation trend.

The SEM images that represent the cell distribution throughout the implant in Figure 15 reveals the cell density in the different groups. The SEM images displaying that the

distribution in every group is equally spread out on the implant surface. The similarities between the cell proliferation and collagen production results are reflected to some extent. The cell density in A10F50 compared to A20F50 differs slightly, especially when comparing the images closest to the wire, Figure 15a versus 15e. When looking at A10F50 compared to the preculture group, the cell density seems to be equal to each other, which does not agree when comparing the cell counts for those groups. The same goes for group A20F50, where the cell density looks higher in the images in Figure 15e-h versus the images representing the preculture in Figure 15q-t, whereas the proliferation results showed a smaller number of cells in A20F50 compared to the preculture group. Those dissimilarities can be caused by differences between replicates in each group or by images not taken in the exact same position. In group A10F50, replicate 8 has a higher cell count compared to replicate 6 and 7, 27200 versus 10800 and 10000. The replicate that was chosen for SEM imaging could have had a cell count closer to replicate 8 than 6 or 7. In that case the cell density should be similar to the preculture group, which can explain the similarities between A10F50 and preculture. The cell count values for replicate 12 and 13 in A20F50 are similar to the mean of the preculture group. In this case the SEM image for preculture can have been in the lower range of preculturing, around 20000 cells, and the cell count for the A20F50 in the upper range of the group.

SEM images for group A50F50, Figure 15i-l, display a cell density that is evidently lower than the preculture group, which is consistent with the proliferation results. The A20F100 group is as well consistent with the proliferation results, since the SEM images in Figure 15m-p are showing a higher cell density in every image compared to the preculture group.

When looking at the morphology of the cells, see Figures 16a, 17a, 18a, 19a, the cells have a spider-web-like structure where the cells are stretched out on the implant surface. The cell morphology is equal between the groups and there is no group where the cell morphology stands out compared to the preculture or the other stimulated groups. This indicates that the electrical stimulation does not impact the cell morphology compared to the preculture, and that the different parameter values do not have a visual impact compared to each other. Furthermore, the cellular attachment is displayed in the different groups in Figures 16b, 17b, 18b, 19b and 20b-d. The attachment in the stimulated groups have similar thread-like parts that integrate with the implant surface. In the preculture group, the thread-like parts were seen on the cell surface, which is displayed in Figure 20c and d. The preculture group was cultured for 16 h, hence the short amount of time could be an explanation to why those threads were not integrated with the surface.

In the stimulated groups a matrix-like structure was discovered, especially in the A20F50 group. Figure 17c shows an osteoblast that is covered in a structured network, where Figure 17d shows an SEM image of the matrix structure with higher magnification. These structures look similar to extra cellular matrix (ECM) structure, which mostly consists of collagen. The matrix structure was also found in the other stimulated groups, but not in the same amount, see Figure 16c, d, 18d and 19d. Since no SEM imaging was performed on a control sample, it is impossible to draw any conclusions that the pulse stimulation increases ECM production. However, the images indicate that applying an amplitude of 20 μA increases the ECM production compared to 10 μA and 50 μA, and that frequency 50 Hz indicates a higher ECM production than a frequency of 100 Hz.

5 Conclusion

In summary, pulsed electrical stimulation exhibited strong positive influence on osteoblast proliferation, collagen production, attachment and spreading on Ti6Al4V surfaces, which are important processes in osseointegration. Research results showed enhanced cell proliferation with current stimulation from 10–50 μA and bone cells grew in higher numbers on stimulated Ti6Al4V as compared to non-stimulated Ti6Al4V surfaces. Among all test conditions, 20 μA indicated as the most beneficial amplitude, although not significantly higher compared to 10 μA and 50 μA. 100 Hz was found to favour cell proliferation and collagen production compared to 50 Hz and the control. The highest osteoblast density was measured at 20 μA and 100 Hz after 72 h where cells grew almost 120% higher in number and 5 times more collagen production as compared to non-stimulated surfaces. Therefore, it can be concluded that pulsed electrical stimulation with similar properties as peripheral nerve stimulation to restore sensory feedback in artificial limbs has a beneficial impact on osteoblast function (e.g., cell survival and collagen production), which may have significant implications for promoting osseointegration compared to non-stimulated surfaces. Furthermore, various amplitude values do not have a significant difference in cell proliferation according to the results, while amplitude 20 μA and 50 μA have a significant higher increase in collagen production compared to 10 μA and non-stimulated surfaces. In addition, higher applied frequency shows a significantly higher cell proliferation and production of collagen.

References

[1] P. I. Brånemark, B. O. Hansson, R. Adell, U. Breine, J. Lindström, O. Hallén, and A. Ohman, "Osseointegrated implants in the treatment of the edentulous jaw. Experience from a 10-year period," *Scand J Plast Reconstr Surg*, vol. 16, pp. 1–132, 1977. [Online]. Available: https://pubmed.ncbi.nlm.nih.gov/356184/.

[2] A. Thesleff, R. Brånemark, B. Håkansson, and M. Ortiz-Catalan, "Biomechanical Characterisation of Bone-anchored Implant Systems for Amputation Limb Prostheses: A Systematic Review," vol. 46, no. 3, pp. 377–391, Mar. 2018, ISSN: 15739686. DOI: 10.1007/s10439-017-1976-4.

[3] K. Pałka and R. Pokrowiecki, "Porous Titanium Implants: A Review," *Advanced Engineering Materials*, vol. 20, no. 5, p. 1 700 648, May 2018, ISSN: 14381656. DOI: 10.1002/adem.201700648. [Online]. Available: http://doi.wiley.com/10.1002/adem.201700648.

[4] M. T. Ehrensberger, C. M. Clark, M. K. Canty, and E. P. McDermott, "Electrochemical methods to enhance osseointegrated prostheses," *Biomedical Engineering Letters*, 2019, ISSN: 2093-985X. DOI: 10.1007/s13534-019-00134-8. [Online]. Available: https://doi.org/10.1007/s13534-019-00134-8.

[5] Y. Li and R. Brånemark, "Osseointegrierte Prothesen zur Rehabilitation nach Amputation: Das wegweisende schwedische Modell," *Unfallchirurg*, vol. 120, no. 4, pp. 285–292, Apr. 2017, ISSN: 01775537. DOI: 10.1007/s00113-017-0331-4. [Online]. Available: https://link.springer.com/article/10.1007/s00113-017-0331-4.

[6] S. Bodhak, S. Bose, W. C. Kinsel, and A. Bandyopadhyay, "Investigation of in vitro bone cell adhesion and proliferation on Ti using direct current stimulation," *Materials Science and Engineering C*, vol. 32, no. 8, pp. 2163–2168, Dec. 2012, ISSN: 09284931. DOI: 10.1016/j.msec.2012.05.032.

[7] A. T. Sidambe, *Biocompatibility of advanced manufactured titanium implants-A review*, 2014. DOI: 10.3390/ma7128168. [Online]. Available: /pmc/articles/PMC5456424/?report=abstract%20https://www.ncbi.nlm.nih.gov/pmc/articles/PMC5456424/.

[8] R. Brånemark, ; P.-I. Brånemark, B. Rydevik, and R. R. Myers, "Osseointegration in skeletal reconstruction and rehabilitation: A review and the VA San Diego Healthcare System," *Journal of Rehabilitation Research and Development*, vol. 38, pp. 175–181, 2001.

[9] J. K. Song, T. H. Cho, H. Pan, Y. M. Song, I. S. Kim, T. H. Lee, S. J. Hwang, and S. J. Kim, "An electronic device for accelerating bone formation in tissues surrounding a dental implant," *Bioelectromagnetics*, vol. 30, no. 5, pp. 374–384, 2009, ISSN: 01978462. DOI: 10.1002/bem.20482.

[10] G. Dergin, M. Akta, B. Gürsoy, Y. Devecioglu, M. Kürkçü, and E. Benlidayi, "Direct current electric stimulation in implant osseointegration: An experimental animal study with sheep," *Journal of Oral Implantology*, vol. 39, no. 6, pp. 671–679, Dec. 2013, ISSN: 01606972. DOI: 10.1563/AAID-JOI-D-10-00172.

[11] C. M. Clark, "Electrochemical Methods for Biofilm Detection and Characterization of Electrically Stimulated Orthopedic Biomaterials," Ph.D. dissertation, University of Buffalo, State University of New York, 2020, p. 246.

[12] W. Wang and J. P. Lynch, "Quantitative assessment of compress-type osseointegrated prosthetic implants in human bone using electromechanical impedance spectroscopic methods," *Biomedical Engineering Letters*, 2019, ISSN: 2093985X. DOI: 10.1007/s13534-019-00139-3.

[13] T. J. Dauben, J. Ziebart, T. Bender, S. Zaatreh, B. Kreikemeyer, and R. Bader, "A Novel in Vitro System for Comparative Analyses of Bone Cells and Bacteria under Electrical Stimulation," *BioMed Research International*, vol. 2016, 2016, ISSN: 23146141. DOI: 10.1155/2016/5178640.

[14] F. G. Zeng, S. Rebscher, W. Harrison, X. Sun, and H. Feng, "Cochlear Implants: System Design, Integration, and Evaluation," *IEEE Reviews in Biomedical Engineering*, vol. 1, pp. 115–142, 2008, ISSN: 19411189. DOI: 10.1109/RBME.2008.2008250.

[15] L. C. Kloth, "Electrical Stimulation Technologies for Wound Healing," *Advances in Wound Care*, vol. 3, no. 2, pp. 81–90, Feb. 2014, ISSN: 2162-1918. DOI: 10.1089/wound.2013.0459. [Online]. Available: http://www.liebertpub.com/doi/10.1089/wound.2013.0459.

[16] M. OrtizCatalan, E. Mastinu, P. Sassu, O. Aszmann, and R. Brånemark, "Self-contained neuromusculoskeletal arm prostheses," *New England Journal of Medicine*, vol. 382, no. 18, pp. 1732–1738, Apr. 2020, ISSN: 15334406. DOI: 10.1056/NEJMoa1917537. [Online]. Available: http://www.nejm.org/doi/10.1056/NEJMoa1917537.

[17] B. M. Isaacson, L. B. Brunker, A. A. Brown, J. P. Beck, G. L. Burns, and R. D. Bloebaum, "An evaluation of electrical stimulation for improving periprosthetic attachment," *Journal of Biomedical Materials Research - Part B Applied Biomaterials*, vol. 97 B, no. 1, pp. 190–200, 2011, ISSN: 15524973. DOI: 10.1002/jbm.b.31803.

[18] F. Buch, T. Albrektsson, and E. Herbst, "Direct current influence on bone formation in titanium implants," *Biomaterials*, vol. 5, no. 6, pp. 341–346, 1984, ISSN: 01429612. DOI: 10.1016/0142-9612(84)90032-2.

[19] L. M. Bins-Ely, E. B. Cordero, J. C. Souza, W. Teughels, C. A. Benfatti, and R. S. Magini, "In vivo electrical application on titanium implants stimulating bone formation," *Journal of Periodontal Research*, vol. 52, no. 3, pp. 479–484, 2017, ISSN: 16000765. DOI: 10.1111/jre.12413.

[20] R. A. Gittens, R. Olivares-navarrete, R. Rettew, R. J. Butera, F. M. Alamgir, B. D. Boyan, and Z. Schwartz, "Electrical Polarization of Titanium Surfaces for the Enhancement of Osteoblast Differentiation," vol. 612, no. August 2012, pp. 599–612, 2013. DOI: 10.1002/bem.21810.

[21] I. S. Kim, J. K. Song, Y. L. Zhang, T. H. Lee, T. H. Cho, Y. M. Song, D. K. Kim, S. J. Kim, and S. J. Hwang, "Biphasic electric current stimulates proliferation and induces VEGF production in osteoblasts," *Biochimica et Biophysica Acta - Molecular Cell Research*, vol. 1763, no. 9, pp. 907–916, 2006, ISSN: 01674889. DOI: 10.1016/j.bbamcr.2006.06.007.

[22] C. F. Arias, M. A. Herrero, L. F. Echeverri, G. E. Oleaga, and J. M. López, "Bone remodeling: A tissue-level process emerging from cell-level molecular algorithms," *PLoS ONE*, vol. 13, no. 9, Sep. 2018, ISSN: 19326203. DOI: 10.1371/journal.pone.0204171.

[23] A. Augustyn, P. Bauer, B. Duignan, A. Eldridge, E. Gregersen, J. Luebering, A. McKenna, M. Petruzzello, J. P. Rafferty, M. Ray, K. Rogers, A. Tikkanen, J. Wallenfeldt, A. Zeidan, and A. Zelazko, *Bone remodeling*, May 28, 2020. [Online]. Available: https://www.britannica.com/science/bone-remodeling.

[24] A. Augustyn, P. Bauer, B. Duignan, A. Eldridge, E. Gregersen, J. Luebering, A. McKenna, M. Petruzzello, J. P. Rafferty, M. Ray, K. Rogers, A. Tikkanen, J. Wallenfeldt, A. Zeidan, and A. Zelazko, *Osteoblast*, Jul. 8, 2020. [Online]. Available: https://www.britannica.com/science/osteoblast.

[25] E. Pettersen, 2020.

[26] Integrum, *Integrum's history*, Feb. 24, 2020. [Online]. Available: https://integrum.se/about-us/integrum-history/.

[27] M. Ortiz-Catalan, B. Hakansson, and R. Branemark, "An osseointegrated human-machine gateway for long-term sensory feedback and motor control of artificial limbs," *Science Translational Medicine*, vol. 6, no. 257, Oct. 2014, ISSN: 19466242. DOI: 10.1126/scitranslmed.3008933. [Online]. Available: https://pubmed.ncbi.nlm.nih.gov/25298322/.

[28] Integrum, *Upgrade your OPRA™ Implant System to e-OPRA*, Jul. 8, 2020. [Online]. Available: https://integrum.se/opra-implant-system/e-opra/.

[29] C. Günter, J. Delbeke, and M. Ortiz-Catalan, *Safety of long-term electrical peripheral nerve stimulation: Review of the state of the art*, Jan. 2019. DOI: 10.1186/s12984-018-0474-8. [Online]. Available: https://doi.org/10.1186/s12984-018-0474-8.

[30] M. Hronik-Tupaj, W. L. Rice, M. Cronin-Golomb, D. L. Kaplan, and I. Georgakoudi, "Osteoblastic differentiation and stress response of human mesenchymal stem cells exposed to alternating current electric fields," *BioMedical Engineering OnLine*, vol. 10, no. 1, p. 9, 2011, ISSN: 1475-925X. DOI: 10.1186/1475-925X-10-9. [Online]. Available: http://biomedical-engineering-online.biomedcentral.com/articles/10.1186/1475-925X-10-9.

[31] "X-Ray Data Booklet Table 1-2. Photon energies, in electron volts, of principal K-, L-, and M-shell emission lines," Tech. Rep. [Online]. Available: https://xdb.lbl.gov/Section1/Table_1-2.pdf.

[32] R. Krämer, "Secretion of amino acids by bacteria: Physiology and mechanism," *FEMS Microbiology Reviews*, vol. 13, no. 1, pp. 75–93, Jan. 1994, ISSN: 01686445. DOI: 10.1111/j.1574-6976.1994.tb00036.x. [Online]. Available: https://academic.oup.com/femsre/article-lookup/doi/10.1111/j.1574-6976.1994.tb00036.x.

[33] J. Hayes, "Osteoblast models for matrix research," *European Cells and Materials*, vol. 24, no. 2012, pp. 1–17, 2012, ISSN: 1473-2262. DOI: 10.22203/eCM.v024a01. [Online]. Available: www.ecmjournal.org.

[34] Chemometec, *NucleoCounter® NC-200™*, Jul. 9, 2020. [Online]. Available: https://chemometec.com/cell-counters/automated-cell-counter-nc-200/.

Appendix

A Protocols

A.1 Protocol for Cleaning and Sterilising Implants and Electrodes

Work solution: 15 mL Extran (MA 02, Merck) + 600 mL deionised water (heated to 70 °C)

1. Place the implants and the electrodes one by one in separated cleaned glass tubes
2. Rinse 2 x 5 min in work solution in an ultrasonic bath at 70 °C
3. Rinse 3 x 5 min in Milli-Q water in an ultrasonic bath
4. Repeat step 2 and 3
5. 2 x rinse with 70 % ethanol
6. Let dry in a sterile hood
7. Place the implants and the electrodes in sterile bags and enclosure with autoclaving tape (one implant or electrode per bag)
8. Autoclave for 20 min in 121 °C

A.2 Protocol for Cleaning and Sterilising Containers

Work solution: 15 mL Extran (MA 02, Merck)+ 600 mL deionised water

1. Place the experimental containers in glass containers
2. Rinse 5 min in work solution in an ultrasonic bath with cold water
3. Rinse 2 x 5 min in Milli-Q water in an ultrasonic bath with cold water
4. Let the containers dry in a sterile fume hood
5. Place the containers in a sterile bag (one container per bag)
6. Place the bags under a UV lamp for 25 min

A.3 Protocol for Measuring Level of Collagen

To measure the level of soluble collagen production in the cell culture medium after the experimental cycle, the Sircol soluble collagen assay from Biocolor was used by following these instructions.

Preparations

1. Reagent blanks - 100 μl fresh cell culture media, the same as used in the experiments.
2. Collagen standards - use aliquots containing 5, 10 and 15 μg of the Collagen Reference Standard. Make each standard up to 100 μl using the same solvent as in reagent blanks.

Assay

1. To each tube add 1 ml of Sircol Dye Reagent. (1 ml of dye is required to fully saturate the collagen molecules within a 100 μl sample volume.)
2. Cap tubes; mix by inverting contents and place tubes in a gentle mechanical shaker for 30 min. (During this time period a collagen-dye complex will form and precipitate out from the soluble unbound dye.)
3. Transfer the tubes to a microcentrifuge and spin at 12000 r.p.m. for 10 min. Carefully invert and drain tubes.
4. Gently layer on 750 μl ice-cold Acid-Salt Wash Reagent to the collagen-dye pellet to remove unbound dye from the surface of the pellet and the inside surface of the microcentrifuge tube.
5. Centrifuge at 12000 r.p.m. for 10 min and drain the wash into a waste container.
6. Add 250 μl Alkali Reagent to reagent blanks, standards and samples.
7. Recap tubes and release the collagen bound dye into the solution. A vortex mixer is suitable.
8. When all of the bound dye has been dissolved, usually within 5 min, the samples are ready for measurement.
9. Transfer 200 μl of each sample to individual wells of 96 micro well plate.
10. Set the microplate reader to 555 nm.
11. Measure the absorbance.

B Results

B.1 Cell Proliferation Preculture

Table 3: Number of cells attached to the implant after 16 hours of preculturing, counted by the NucleoCounter.

Replicate	Counted cells	Mean (counted cells)
P1	20000	24600
P2	25600	
P3	26800	
P4	22400	
P5	26000	
P6	26800	

B.2 Cell Proliferation Image Analysis

Control

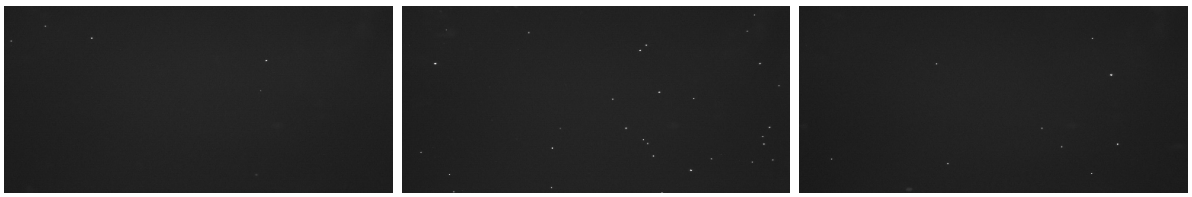

(a) Replicate 1, <5000 **(b)** Replicate 2, 5600 **(c)** Replicate 3, <5000

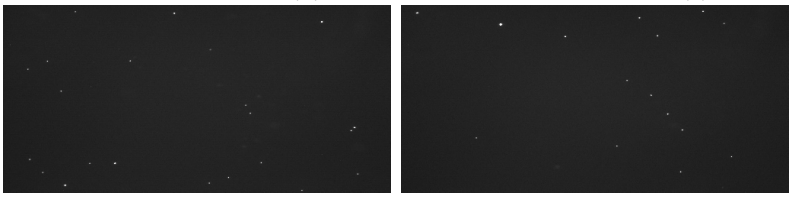

(d) Replicate 4, 4000 **(e)** Replicate 5, 2800

Figure 21: Images provided by the NucleoCounter view for replicate a) 1, b) 2, c) 3, d) 4 and e) 5.

A10F50

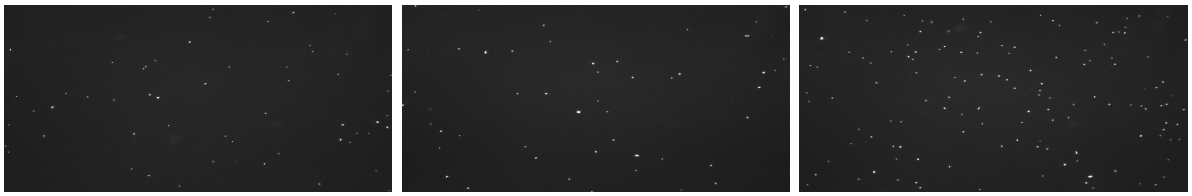

(a) Replicate 6, 10800 **(b)** Replicate 7, 10000 **(c)** Replicate 8, 27400

Figure 22: Images provided by the NucleoCounter view for replicate a) 6, b) 7 and c) 8.

A20F50

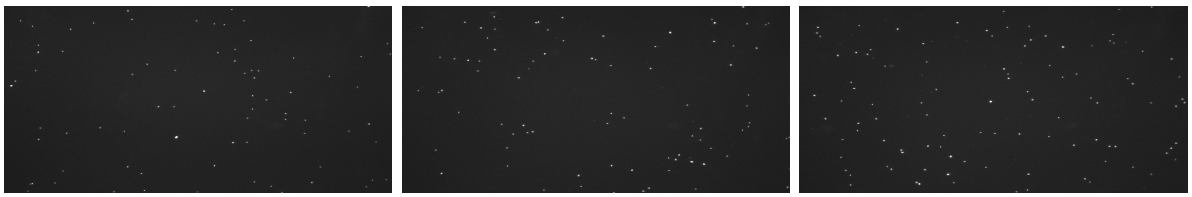

(a) Replicate 11, 13600 **(b)** Replicate 12, 20400 **(c)** Replicate 13, 21600

Figure 23: Images provided by the NucleoCounter view for replicate a) 11, b) 12 and c) 13.

A50F50

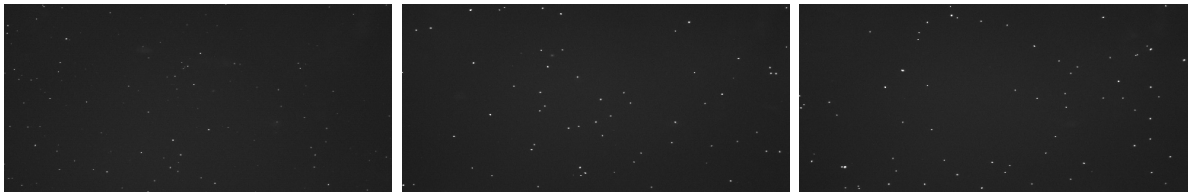

(a) Replicate 16, 10400 **(b)** Replicate 17, 11600 **(c)** Replicate 18, 13200

Figure 24: Images provided by the NucleoCounter view for replicate a) 16, b) 17 and c) 18.

A20F100

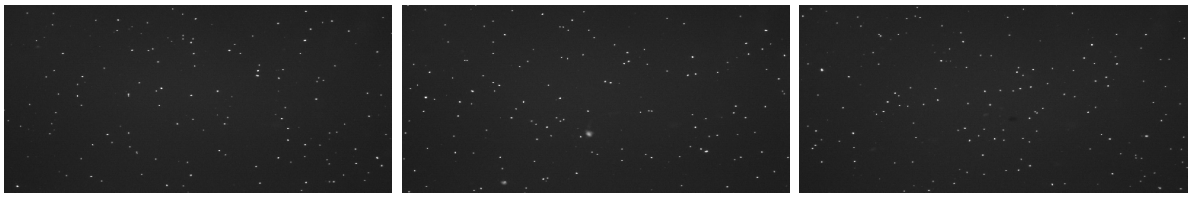

(a) Replicate 21, 26800 **(b)** Replicate 22, 28800 **(c)** Replicate 23, 30400

Figure 25: Images provided by the NucleoCounter view for replicate a) 21, b) 22 and c) 23.

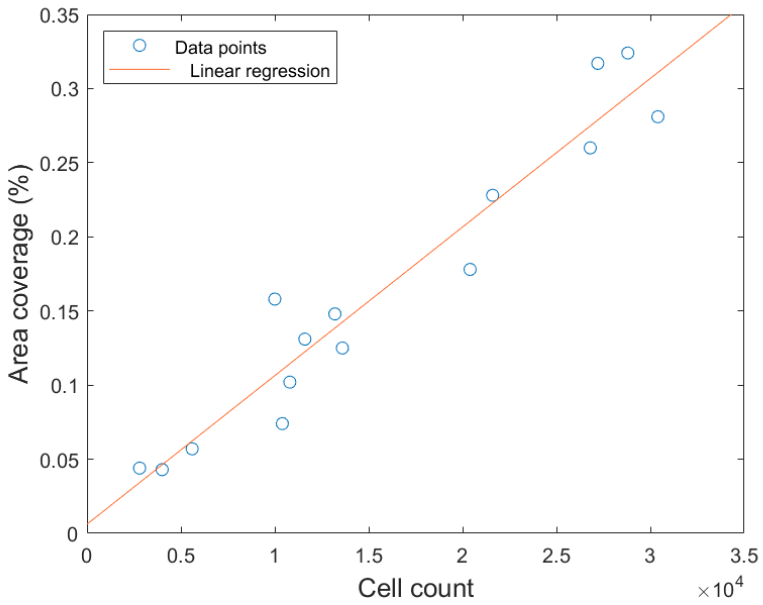

Figure 26: Area coverage of fluorescent image provided by the NucleoCounter plotted against the cell count. The linear regression has a function of $y = 1.0002E^{-05x} + 0.006176$ with $R^2 = 0.9296$ and $p < 0.05$.

B.3 Raw Data Cell Proliferation

Table 4: Number of counted cells by the NucleoCounter for each replicate in every group, as well as the normalised proliferation value against the mean value of the preculture. The calculated area coverage from the provided images from the NucleoCounter. Note, * is the estimated value from the image analysis and not the cell count value provided by the NucleoCounter.

Group	**Replicate**	**Cell count**	**Cell proliferation**	**Area coverage (%)**
Control	1	500*	0.020	0.011
	2	5600	0.228	0.057
	3	1900*	0.077	0.025
	4	4000	0.163	0.043
	5	2800	0.114	0.044
A10F50	6	10800	0.439	0.102
	7	10000	0.407	0.158
	8	27200	1.106	0.317
A20F50	11	13600	0.553	0.125
	12	21600	0.878	0.228
	13	20400	0.829	0.178
A50F50	16	10400	0.423	0.074
	17	11600	0.472	0.131
	18	13200	0.537	0.148
A20F100	21	26800	1.089	0.260
	22	28800	1.171	0.324
	23	30400	1.236	0.281

B.4 Raw Data Collagen Production

Table 5: Raw data from absorbance measurements at 555 nm presented as the collagen production in μg, where the replicate mean and group mean are calculated as well.

Group	Replicate	Technical replicate	Collagen (μg)	Replicate mean (μg)	Group mean (μg)
Control	1	1:1	0.033	0.353 ±0.280	1.384 ±1.145
		1:2	0.471		
		1:3	0.0.554		
	2	2:1	2.275	1.997 ±1.073	
		2:2	2.904		
		2:3	0.812		
	3	3:1	1.280	2.411 ±1.392	
		3:2	3.965		
		3:3	1.986		
	4	4:1	2.265	1.1822 ±0.534	
		4:2	1.229		
		4:3	1.971		
	5	5:1	0.234	0.338 ±0.244	
		5:2	0.162		
		5:3	0.616		
A10F50	6	6:1	1.095	1.744 ±1.129	1.646 ±0.853
		6:2	1.090		
		6:3	3.048		
	7	7:1	1.729	1.909 ±0.161	
		7:2	2.038		
		7:3	1.961		
	8	8:1	1.080	0.918 ±0.684	
		8:2	0.167		
		8:3	1.507		
	9	9:1	1.280	1.243 ±0.414	
		9:2	1.636		
		9:3	0.812		
	10	10:1	2.378	2.418 ±1.049	
		10:2	1.389		
		10:3	3.486		

Table 6: Continued.

Group	Replicate	Technical replicate	Collagen (μg)	Replicate mean (μg)	Group mean (μg)
A20F50	11	11:1	0.301	1.655 ±1.174	3.845 ±2.182
		11:2	2.275		
		11:3	2.388		
	12	12:1	0.611	1.962 ±1.498	
		12:2	3.573		
		12:3	1.703		
	13	13:1	6.382	5.842 ±0.715	
		13:2	6.114		
		13:3	5.032		
	14	14:1	2.605	4.800 ±2.638	
		14:2	7.727		
		14:3	4.068		
	15	15:1	4.352	4.814 ±0.984	
		15:2	4.145		
		15:3	5.944		
A50F50	16	16:1	2.239	2.953 ±0.674	3.261 ±1.273
		16:2	3.579		
		16:3	3.043		
	17	17:1	2.780	4.374 ±1.460	
		17:2	5.645		
		17:3	4.697		
	18	18:1	1.930	3.391 ±1.329	
		18:2	4.527		
		18:3	3.718		
	19	19:1	2.976	3.513 ±1.499	
		19:2	2.357		
		19:3	5.207		
	20	20:1	2.744	2.072 ±0.706	
		20:2	2.136		
		20:3	1.337		
A20F100	21	21:1	4.398	5.908 ±1.641	5.929 ±1.794
		21:2	5.671		
		21:3	7.654		
	22	22:1	6.732	5.052 ±1.633	
		22:2	4.954		
		22:3	3.470		
	23	23:1	5.284	5.961 ±1.668	
		23:2	4.738		
		23:3	7.861		
	24	24:1	4.176	4.317 ±0.262	
		24:2	4.156		
		24:3	4.619		
	25	25:1	8.263	8.409 ±0.198	
		25:2	8.263		
		25:3	8.330		

C Article draft

Promoting osseointegration with electrical stimulation: a review

Emily Pettersen[1,2], Max Ortiz Catalan[1,2,3,4]

[1]Center for Bionics and Pain Research, Sweden.

[2]Department of Electrical Engineering, Chalmers University of Technology, Sweden.

[3]Operational Area 3, Sahlgrenska University Hospital, Sweden.

[4]Department of Orthopaedics, Institute of Clinical Sciences, Sahlgrenska Academy, University of Gothenburg, Sweden.

Abstract

Electrical stimulation has shown to be a potential approach for promoting osseointegration in bone-anchored implants, where osseointegration defines the biological bonding between an implant surface and bone tissue. Inadequate osseointegration is one of the major factors of implant failure, which in the worst case leads to implant removal and shortening of the residual limb. The concept of enhancing biofunctionality at the implant-bone interface with electrical stimulation for reducing healing time and increasing implant's lifespan has been tested in different models, both *in vitro* and *in vivo*, with various approaches ranging from different configurations to current sources and electrical stimulation parameters. However, optimal stimulation parameters have not been thoroughly investigated.

This review compare and contrast 13 published studies from the last 45 years that have investigated electrical stimulation modalities as a means to promote osseointegration, with a focus on the electrical stimulation parameters used. The reviewed studies utilized nonuniform protocols with disparities in cell type and species/animal model, implant location, experimental timeline, implant material, evaluation assays and applied electrical stimulation. However, *in vitro* models showed that

osteoblasts were sensitive to current/voltage magnitude, stimulation duration as well as the stimulation treatment, likewise for bone quantity around implants in *in vivo* applications. The reviewed studies reflect a gap between *in vitro* and *in vivo* studies. Despite *in vitro* results indicating certain beneficial stimulation parameter values, amplitude magnitude of 15-25 µA, *in vivo* studies have been performed afterwards with too low magnitude, 7.5 µA. In conclusion, electrical stimulation has shown to have potential for promoting ossoeintegration and to reach a clinical setting, further investigations regarding optimising the electrical stimulation parameters is needed.

Keywords: osseointegration, DC stimulation, titanium implant, bone formation, prostheses

1 Background

The discovery of osseointegration, the natural phenomenon that defines the process of biological bonding between an implant surface and bone tissue [1], revolutionised the application of limb prostheses by providing the means to skeletal attachment [2] and thus allowing for mechanical coupling and load transfer [3]. The osseointegrated prosthesis has increased the quality of life for people with amputations by exceeding limitations with conventional socket prostheses such as skin irritations and nerve compression, and allowing for control of the artificial limb and restoration of sensory and tactile perception [4]. It has been suggested that in order to obtain a successful osseointegrated prosthesis, the bone-implant interface must be achieved rapidly, be properly maintained, and remain free from infections [4]. Inadequate osseointegration is one of the major factors of implant failure, which in the worst case can lead to implant removal and shortening of the residual limb [2]. Furthermore, there is a large risk for bacteria attachment and biofilm formation on the surface which can emerge several years after implantation and potentially cause major infections [5]. Another result of failed osseointegration is implant loosening, when the implant is not properly anchored in the bone tissue and the implants cannot perform in the way they should [6]. The osseointegration process can take up to several months depending on the implant design. In situations

where early loading of the implant is desired, or when the implant is placed in weakened bone, there is a need to stimulate the osseointegration process to a rapid and potentially better completion [7] [8].

The concept of enhancing the biological bonding between the implant and bone tissue has been widely investigated including developing and implementing surface modifications, implant designs, implant materials and surgical implantation techniques [9]. This review aims to compare and contrast published studies from the last 45 years that have investigated electrical stimulation (ES) modalities as a means to promote osseointegration, with a focus on the ES parameters used. Applications using the implant as a stimulating electrode and titanium as the implant material due to its corrosion resistance and mechanical strength received specific emphasis during the literature search process. Emphasis was also given to applications that primarily investigated the effect of ES and not in combination with another approach, e.g., mechanical stimuli or surface modifications. Peer-reviewed publications were identified in PubMed, Google Scholar and the Chalmers University of Technology Library using the keywords: osseointegration, electrical stimulation, direct current stimulation, titanium implant, bone formation.

2 Promoting osseointegration with electrical stimulation

The use of ES to promote osseointegration has been explored over the past decades in both *in vitro* and *in vivo* models, with various approaches ranging from different electrode configurations and ES parameters to sources of current. Electrically stimulated bone growth was originally described by Fukanda *et al.* (1957) [10] for enhancement of osteogenesis in fracture healing, where they exhorted that electrical fields were generated by mechanical stress on bone. In turn, these forces compress the tubular structure of bone and cause fluid flow containing ions through the canalicular system, which stimulated bone healing. In other terms, when a force is applied to the bone, electrical signals are generated due to the ion flow and those signals can be explained by the piezoelectric theory [8]. ES has been successfully applied in a clinical setting to promote osteogenesis [11], bone formation [12]

and for treatment of non-union bone fractures [13], with mainly three modalities: direct current, capacitive coupling and inductive coupling [14]. Some studies have also shown that ES has a positive effect on osseointegration [4]. However, the underlying pathway in the occurrence of the enhanced osseointegration is yet undiscovered and the ideal ES parameters with the greatest impact remains undefined [4].

Before reviewing, it is central to emphasise the basic differences between using ES to promote osteogenesis in bone fraction healing compared to promoting osseointegration in bone-anchored implants. In osteogenesis applications, the current is delivered through cathodic stainless-steel wires which are located near the fracture site to enhance the bone formation from one bone segment to another [4]. This is performed without any prior electrode-bone interface. In osseointegration applications, the current is delivered through the implant to enhance the biological bonding between the implant surface and the surrounding bone. In this manner, the interference regarding the electrochemical properties and the biological bonding between the implant and the adjacent microenvironment is of highest interest [4].

2.1 Electrode configuration, sources and parameters

There exist few ways to provide an electric field (EF) based on the configuration of the electrodes and the electrical source when promoting osseointegration with ES. Briefly, voltage (V) describes the electromotive force (EMF) that has the capacity to move charged particles across the cell membrane in body tissue and EMF is needed to drive a current (1 A) through a resistance (1 Ω). The relationship between the voltage and current is described by Ohm's law: U=RI [15]. To create an EF over a tissue, a source with free electrons is needed in order to transmit current via the patient's tissue or bone through conductive electrodes, positioned to distribute a flow of charged particles over the area where osseointegration is desired [15].

Electrode configuration

The location of the electrodes impacts the outcome of the EF and the stimulation can either be endogenous or exogenous. Stimulation with an exogenous configuration uses the implant fixture as the cathode whereas the anode electrode is placed externally on the skin (Figure 1). The externally placed electrode can be of different types, e.g., ring electrodes which enclose the residual limb [16] or incorporated in an electrical stimulator attached to, e.g., a dental implant abutment [7]. Endogenous stimulation implies that the electrodes are placed internally, either in the bone or in other soft tissues such as muscles or fat. The majority of *in vivo* studies have used the implant that is incorporated in the bone tissue as the cathode and the other electrode placed in tissue nearby as the anode [4].

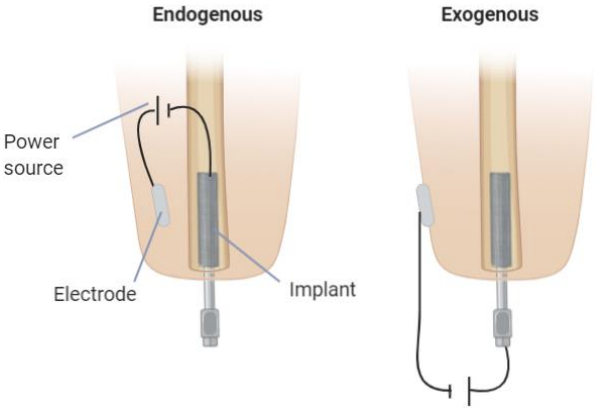

Figure 1. Endogenous vs exogenous electrode configurations for electrical stimulation.

Electrical stimulation sources

Electrical current defines the rate of flow of charged particles past a specific point and in specific direction [15]. The flow of current in a wire occurs due to movement of free electrons, whereas the current flow in body tissue arises when ions such as K^+, Na^+ and Cl^- are moving across the cell membrane. Two main sources provide an electrical current: direct current (DC) and alternating current (AC). DC is the current that passages continuously during a set period with the same direction, while in AC the direction of the moving charged particles fluctuates over time. Pulsed current is an isolated electrical event where charged particles flow either unidirectionally or bidirectionally [15]. Each event is called a pulse and pulses are separated by a longer period of time

where no current flows at all. The pulse repeats itself in a series during an infinite time span [15]. Pulses can be created in several ways combining different shapes and waveforms. For example, a pulse can be rectangular with a monophasic waveform above the zero baseline (Figure 2A). If the pulse is above the baseline it has positive polarity. Moreover, the pulse can take a biphasic waveform, where the pulse crosses the zero baseline to appear both above and below. The pulse shape can either be symmetric (Figure 2B) and charged balanced without polarity or asymmetric (Figure 2C) and charged unbalanced with polarity. In addition to shape, waveform and polarity, negative and positive amplitude (µA), frequency (Hz), pulse width (µs), inter-pulse-break (µs) and polarity (%) are parameters that need to be set. Each change of property or parameter causes a different outcome.

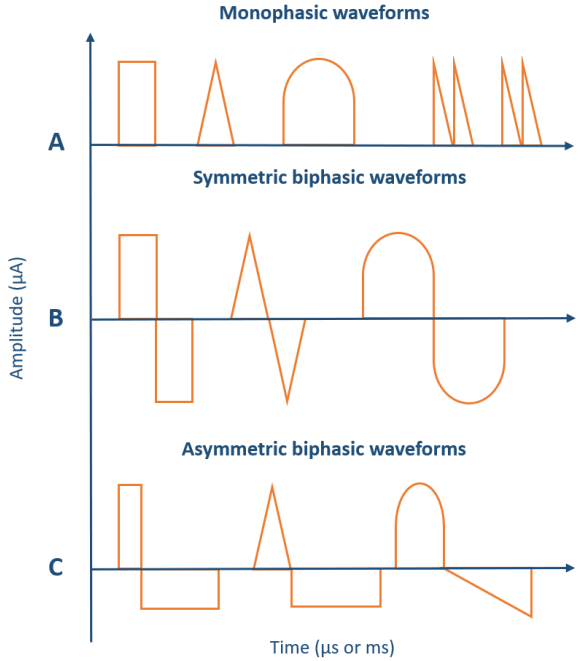

Figure 2. Pulsed electrical current can have many different shapes and waveforms. ***A)*** *Examples of monophasic waveforms above the zero baseline. If the pulse is above the baseline it has positive polarity and if the pulse is below baseline it has negative polarity.* ***B)*** *and* ***C)*** *Examples of biphasic waveforms. The pulse crosses the zero baseline to appear both above and below the baseline. The pulse shape may be symmetric* ***B)*** *and charged balanced without polarity or asymmetric* ***C)*** *and charged unbalanced with polarity.*

2.2 DC stimulation

The most studied technique of stimulation in both *in vitro* and *in vivo* applications is the invasive DC stimulation. DC stimulation has been shown to have a positive impact on osteoblast functions as well

as to lead to an improved bone-to-implant interface [4]. Despite beneficial outcomes, there have been some problems associated with the technique. For instance, ES can cause accumulation of charged proteins at the electrode surface of opposite charge, which in turn can obstruct current flow at these locations and result in inconsistent current delivery to the cells [17]. Moreover, it has also been reported that ES can trigger formation of reactive oxygen species (ROS) in forms of hydroxyl, hydrogen peroxide and free radicals [18], and that such ROS have been shown to initiate bone resorption [19]. Constant DC has been suggested to result in increased pH [17], which causes a toxic environment for cells and tissues, but studies have also reported that this environment can stimulate osteoblastic activity [20] [21] [22]. A recently published article by Srirussamee *et al.* (2019) [14] reported that the role of faradic by-products is not dominant in preosteoblast response in terms of Bmp2 and Spp1 mRNA expression, and that the by-products alone are less effective in promoting bone formation without ES. Their results imply that cellular responses from preosteoblasts to ES are predominantly triggered by the mechanism involving EF, potential, and/or current [14]. In conclusion, the underlying mechanism for the beneficial outcomes of DC stimulation is uncertain and must be further investigated.

2.3 Pulsed current stimulation

To overcome some of the addressed problems with constant DC stimulation, a new ES approach including pulsating current was developed in the early 2000s. One early study investigated the effect of biphasic electrical current (BEC), in order to minimise the net charge of accumulation during cell exposure to ES due to its balance charged property [17]. This *in vitro* study, carried out by Kim *et al.* (2006) [17], showed that BEC stimulation induced cell proliferation and vascular endothelial growth factor (VEGF), a marker for angiogenesis [23] . However, no pH or ROS measurements were performed. This research group has further tested BEC stimulation in a canine mandibular model where the chosen parameters in the animal model was based on the *in vitro* results. They reported a significantly increase in bone area (BA) and bone-implant contact (BIC) around stimulated specimens after

3 weeks [7]. The choice of stimulation parameters increases when using pulsating stimulation compared to the constant DC current, which needs to be considered when designing the trials.

2.4 Assessment of osseointegration

Osseointegration is assessed by either *in vitro* or *in vivo* methods. *In vitro* evaluation of osseointegration can be performed by investigation of osteoblast proliferation, viability, function, and attachment, while *in vivo* evaluation involves the use of animal models combined with histological assessments and investigations of local infection or inflammation at the implant site.

The most common assays used in the reviewed *in vitro* studies are presented in Table 1, where the assays are categorised by evaluated cell activity, e.g., measurement of metabolic activity, cell proliferation, cell viability, relevant bone markers such as hormones and growth factors, cellular attachment and morphology. These methods were often used in combination in the reviewed literature, e.g., cell proliferation investigated alongside cellular attachment and a relevant bone marker, to provide a more thorough understanding of the stimulation effect. Numerous evaluation assays are commercially available. Note that one assay can often examine several activities, such as the colorimetric MTT assay that measures metabolic activity via reduction of a yellow tetrazolium salt to purple formazan crystals and thus can be used as an indicator for both cell proliferation and viability [24]. Cell proliferation over a set time period can also be measured by physically removing cells with trypsin-EDTA, then counting the cells with or without assistance of dye or fluorescent imaging [25]. Hormones and growth factors, such as the bone formation and mineralisation marker alkaline phosphate (ALP), can be analysed by enzyme-linked immunosorbent assay (ELISA), radioimmunoassay (RIA), or quantification of RNA transcript levels in cells using reverse transcription polymerase chain reaction (RT-PCR). Qualitative measurements such as scanning electron microscopy (SEM) also enable high magnification imaging for studying cellular attachment and morphology in conjunction with chemical analyses [26].

195 *Table 1. In vitro assessments of osseointegration.*

	Assessment	Assessment description	Outcome measures				
			Cell proliferation	*Cell viability*	*Cell adhesion*	*Cell morphology*	*Bone markers**
Colorimetric assay	MTT[1]	MTT is reduced into fluorescent purple formazan crystals by living cells, which determines mitochondrial activity assisted by a spectrophotometer [27].	X	X			
	WST-1[1]	WST-1 is cleaved to soluble fluorescent formarzan by a complex cellular mechanism that mainly occurs at the cell surface, which determines living cell activity assisted by a spectrophotometer [28].	X	X			
	Resazurin	Resazurin is reduced to strongly-fluorescent resorufin by living cells, which determine mitochondrial activity assisted by a spectrophotometer [27].	X	X			
Staining	LIVE/DEAD	Fluorescent staining of cells using calcein-AM (viable cells), propidium iodide (dead cells) and Hoechst 33342 (total cells) [29].		X			
	Trypan blue	Staining elimination test where viable cells do not take up the dye, but dead cells are permeable to it [29].		X			
Imaging	SEM[3]	Electron microscope that enables high-resolution imaging and generates specimen images by scanning of the surface using a focused beam of electrodes [26].			X	X	
	Fluorescent microscopy	Optical imaging method used to study cell physiology by using fluorescence [30].			X	X	
	CLSM[4]	Optical imaging method used for enhancing optical resolution and contrasting a micrograph by usage of a spatial pinhole to stop out-of-focus light in image formation [31].				X	
PCR methods	RT-PCR[6]	A variation of the standard PCR[5] method where cDNA[7] is made from RNA[8] via reverse transcription, which allows amplification of specific mRNA transcripts from small biological specimens [32].					X
	qPCR[9]	Another variation of standard PCR where two elements are added to the standard procedure: fluorescent dye and fluorometer. Widley used for quantifying RNA transcript levels in cells and tissues [32].					X
	RT-qPCR[10]	A variation of PCR that combines both RT-PCR and qPCR [32].					X
Immunoassays	ELISA[11]	Used for quantification which utilise an antibody labelled with an enzyme marker where either the enzyme or antibody is bound to an immunosorbent substrate. The change in enzyme activity is a result of the enzyme-antibody-antigen reaction which is proportional to the antigen concentration [33].					X
	RIA[12]	Used for quantification of antigen-antibody reaction by usage of a radioactively labelled substance either directly or indirectly to quantify the binding of the unlabelled substance to a specific antibody [34].					X
	Western blotting	Identification assay used to identify proteins or peptides that have been electrophoretically separated via blot relocating from electrophoresis gel into strips of nitrocellulose paper followed by labelling with antibody probes [35].					X

*Common bone markers include alkaline phosphatase (ALP), bone morphogenetic protein 2 (Bmp2), collagen type 1 (Col 1), high-mobility group box 1 (Hmgb1), procollagen type 1, osteoprotegerin (OPG), osteocalcin (OC), secreted phosphoprotein 1 (Spp1), Runt-related transcription factor 2 (Runx2), and vascular endothelial growth factor (VEGF).

[1]**MTT**, 3-(4,5-dimethylthiazol-2-yl)-2,5-diphenyltetrazolium bromide; [2]**WST-1**, 2-(4-Iodophenyl)-3-(4-nitrophenyl)-5-(2,4-disulfophenyl)-2H-tetrazolium; [3]**SEM**, scanning electron microscopy; [4]**CLSM**, confocal laser scanning microscopy; [5]**PCR**, polymerase chain reaction; [6]**RT-PCR**, reverse transcriptase PCR; [7]**cDNA**, complementary DNA; [8]**RNA**, ribonucleic acid; [9]**qPCR**, quantitative PCR; [10]**RT-qPCR**, reverse transcriptase quantitative PCR; [11]**ELISA**, enzyme-linked immunosorbent assay; [12]**RIA**, radioimmunoassay

2.4.1 *In vitro* studies

There are relevant *in vitro* studies reported in the literature which use a model where cells are cultured directly on electrically stimulated cathodes to assess acceleration of osseointegration [17], [36]–[39], (Table 2). Different ES treatments have been investigated in short term studies lasting between 2 hours (h) and 5 days. These studies have shown increased cell growth [17], [38], osteoblastic differentiation [36], [37] and osteoblast attachment [38] on stimulated surfaces compared to non-stimulated surfaces. However, after 24 h of ES at catholically polarised titanium, results have also shown reduction in number of viable cells as well as changed morphology [39].

Some studies have applied a voltage-controlled EF, evaluating both DC and AC voltage. Sivan *et al.* (2013) [39] provided constant catholically polarised surfaces of 300, 350, 400, 450, 500, 600, 1000 mV with MC3T3-E1 cells cultured directly at the titanium (Ti6Al4V) surface. Their results showed that cell viability and morphology were both time- and voltage-dependent; cells transitioned from viable to nonviable after 10 h at -400 mV, 6 h at -500 mV and 2 h at -600 and -1000 mV, and 24 h at -400 mV was detected as a threshold limit for cell apoptosis [39]. Furthermore, Gittens *et al.* (2013) [37] studied differentiation of MG63 cells at catholically polarised surfaces and found a higher rate of differentiation when stimulation was increased from -100 mV to -500 mV in steps of 100 mV. Srirussamee *et al.* (2019) stimulated the osteoblastic cell line MC3T3-E1 for 1 and 2 h, respectively, with a DC voltage of 2.2 V (100 mV/mm equivalent electric field) [14]. Their results showed a greater upregulation of Bmp2 and Spp1 after 2 h ES compared to 1 h ES and non-stimulation, thus implying that the longer ES time was more beneficial than shorter or no ES. Moreover, Dauben *et al.* (2016) [36] developed a novel *in vitro* system where human primary osteoblasts (hPOB) were exposed to voltage-controlled sinusoidal stimulation of 0.2 and 1.4 V_{RMS}, respectively, frequency of 20 Hz and stimulation periods of 3 x 45 min per day with a break of 225 min between each stimulation for 3 days in total. Cells remained viable after the alternating stimulation, but metabolic activity was not significantly higher in stimulated groups compared to controls. However, gene expression showed moderately

higher transcript abundance of ALP, collagen type 1 (Col I) and osteocalcin (OC) after stimulation of 0.2 V_{RMS} compared to controls, and enhanced transcript levels of OC after application of 1.4 V_{RMS} [36].

Current-controlled stimulation has also been investigated with both constant DC and pulses. Bodhak *et al.* (2012) [38] stimulated human foetal osteoblasts (hFOB) with constant DC stimulation of 5, 15 and 25 µA, respectively, for 15 min every 8 h. After 5 days of stimulation, there was a significant increase in cell-material interaction and density of viable cells in stimulated compared to non-stimulated surfaces. There was also a significant increase between the different stimulation conditions, where 25 µA was more favourable compared to 5 and 15 µA. Furthermore, Kim *et al.* (2006) [17] stimulated rat calvarial osteoblasts (rcOB) with biphasic pulses of 20 µA, (1.5 µA/cm^2), pulse width of 32 µs and frequency of 3000 Hz. They studied two different stimulation modes: interrupted (6 h daily) and continuous (24 h daily). A significant increase of cell proliferation was found after 2 days with continuous stimulation compared to interrupted stimulation and non-stimulated surfaces. BEC was also found to increase VEGF production, but did not stimulate osteoblast differentiation [17].

Whilst the reported outcomes in the *in vitro* applications seemingly vary, there are several aspects to emphasise. The *in vitro* studies did not utilise uniform models, where differences in cell type and species (MG63, MC3T3-E1, hPOB, hFOB, rcOB), experimental timeline (stimulation durations relative valuation time points), implant material (Ti, Au, Pt), evaluation assays, and applied ES (magnitude, pattern, duration, control unit) may all have contributed to the disparity in reported results. However, despite differences in the models used, various ES parameters seem to have a vital role for the enhancement of osseointegration. Studies have shown that osteoblast functions are impacted by voltage/current magnitude [38], [36], [37], [39], stimulation duration [14], [17] and treatment duration [39], while other potentially important parameters such as duty cycle, pulse width, and frequency are not comprehensively studied. Furthermore, in the majority of the reviewed studies, motivation behind the selection of ES parameters is absent. For instance, Bodhak *et al.* (2012) [38] stimulated for 15 min

every 8 h, whereas Dauben *et al.* (2016) [36] stimulated for 3 x 45 min daily with a break of 225 min between each stimulation. It is unclear whether the stimulation patterns were selected for scientific reasons, e.g., if one pattern was shown in feasibility studies to be more beneficial than another for promoting osteoblast function, or if they were selected for practical reasons, e.g., due to limitations of the control unit.

Table 1. In vitro studies categorised by cell type, cathode material, evaluation, stimulation parameters, stimulation duration and results.

Reference	Cell type	Cathode material	Evaluation	Stimulation parameters	Stimulation duration	Results
Dauben et al. 2016 [36]	Human primary osteoblast	Ti6Al4V	WST-1[1], LIVE/DEAD staining, RT-PCR[2] (Col I[3], ALP[4], OC[5]), ELISA[6] (procollagen type 1)	0.2 and 1.4 V_{RMS}, frequency of 20 Hz, sinusoidal signal was applied with stimulation periods of 3 × 45 min per day with 225 min break between simulations	3 days	Cells were viable and the metabolic activity was not significantly higher in stimulated groups compared to controls. Gene expression showed moderately higher transcript abundance of Col I, ALP, and OC after electrical stimulation with 0.2 V_{RMS} compared to controls. Application of 1.4 V_{RMS} resulted in slightly enhanced OC transcript levels while Col I and ALP remained unchanged.
Gittens et al. 2013 [37]	Osteoblast (MG63)	Unalloyed Ti, Grade 2 (ASTM F67)	Trypsin, radioimmunoassay (OC), ELISA (OPG[7], VEGF[8])	Anode polarisation of 100 mV and cathode polarisation of 100, 200, 300, 400 and 500 mV	2 h	MG63 differentiation and local factor production was enhanced on catholically polarized surfaces. The effect of the applied electrical polarization was voltage dependent, with higher potentials promoting a greater osteoblast differentiation.
Bodhak et al. 2012 [38]	Human foetal osteoblast (hFOB 1.19)	99.7 % pure Ti, Grade 2	MTT[9], SEM[10], fluorescent staining & CLSM[11] (vinculin expression)	5, 15, 25 µA constant stimulation for 15 min every 8 h	5 days	Enhanced bone cell–material interactions with increasing amount of DC[12] stimulation from 5 µA to 25 µA. The highest viable osteoblast cell density was measured on 25 µA stimulated Ti surface where cells grew almost 30 % higher in number as compared to non-stimulated Ti surface.
Srirussamee et al. 2019 [14]	Preosteoblast (MC3T3-E1)	99.95 % platinum	pH measurements, fluorometric H_2O_2 assay, resazurin assay, mRNA expression RT-qPCR[13] (Hmgb1[14], Bmp2[15], Vegfa[16], Spp1[17], Runx2[18])	1 and 2 h per day with constant DC voltage of 2.2 V (100 mV/mm equivalent electric field)	3 days	No respond of preosteoblasts to faradic by-products in terms of Bmp2 and Spp1. The roles of faradic by-products are not dominant, and the by-products alone are less effective in promoting bone formation without presence of electrical stimulation. Results imply that cellular responses from preosteoblasts to ES are predominantly triggered by the mechanism involving electric field, potential, and/or current.
Sivan et al. 2013 [39]	Preosteoblast (MC3T3-E1)	Ti6Al4V	SEM, LIVE/DEAD staining	Cathode polarisation of 300, 350, 400, 450, 500, 600, 1000 mV (vs Ag/AgCl)	24 h	Cell death at commercially pure titanium is both dependent in cathodic voltage and time. Cell culture above -300 mV showed almost no loss in viability, whereas 100 % of the cells were killed at -600 mV after 24 h.
Kim et al. 2006 [17]	Rat calvarial osteoblast	Au	Trypan blue staining, RT-PCR and qPCR[19], ELISA (VEGF, BMP-2), Western blotting (HIF-1α[20])	BEC[21] stimulation with pulse amplitude of 20 µA (1.5 µA/cm^2), pulse width 32 µs and frequency of 3000 Hz in the interrupted (6 h daily) and continuous mode (24 h daily)	2, 4 and 5 days	Significant increase of cell proliferation after 2 days with stimulation of continuous mode compared to interrupted mode and non-stimulated groups. BEC stimulation increased VEGF production, but did not stimulate differentiation.

[1]**WST-1**, 2-(4-Iodophenyl)-3-(4-nitrophenyl)-5-(2,4-disulfophenyl)-2H-tetrazolium; [2]**RT-PCR**, reverse transcriptase PCR; [3]**Col 1**, collagen type1; [4]**ALP**, alkaline phosphatase; [5]**OC**, osteocalcin; [6]**ELISA**, enzyme-linked immunosorbent assay; [7]**OPG**, osteoprotegerin; [8]**VEGF**, vascular endothelial growth factor; [9]**MTT**, 3-(4,5-dimethylthiazol-2-yl)-2,5-diphenyltetrazolium bromide; [10]**SEM**, scanning electron microscopy; [11]**CLSM**, confocal laser scanning microscopy; [12]**DC**, direct current; [13]**RT-qPCR**, reverse transcription quantitative PCR; [14]**Hmgb1**, high-mobility group box 1; [15]**Bmp2**, bone morphogenetic protein 2; [16]**Vegfa**, vascular endothelial growth factor A; [17]**Spp1**, secreted phosphoprotein 1; [18]**Runx2**, runt-related transcription factor 2; [19]**qPCR**, quantitative PCR; [20]**HIF-1 α**, hypoxia-inducible factor 1-alpha; [21]**BEC**, biphasic electrical current

2.4.2 *In vivo* studies

ES applied directly through the implant to accelerate osseointegration has as well been investigated *in vivo* (Table 3), where several studies have reported promising results [7], [12], [40]–[43]. Both short (1 day [43]) and long term (up to 12 weeks [8]) durations of stimulation have been investigated. Most studies applied a current-controlled EF with a magnitude between 5 to 50 µA. Animal models used include rabbits, dogs, and sheep, and the titanium, Ti6Al4V, or cp Ti grade IV implant was located in the tibia, mandible and femur (Table 3). Evaluations of these *in vivo* studies differed from those used in *in vitro* studies. Primarily bone quality (porosity, density), bone growth at the implant site (including growth rate, necrosis, bone mineral content (BMC) including calcium content and histological assessment of mature or immature bone formation), and degree of skeletal attachment (including histological or SEM assessments such as appositional bone index, bone contact area (BCA), and BIC, as well as mechanical testing) have been assessed.

Isaacson *et al.* (2011) [40] applied an EF with a potential difference of 0.55 V in a rabbit model. The gold coated Ti6Al4V implant was catholically stimulated and placed inside the medullary channel in the femur, and the anode was placed ~1.5 cm from the periosteum in the adjacent musculature. Stimulation was ongoing for 3 and 6 weeks. Histological assessments of appositional bone index and mineral apposition rates were not found to be improved by ES, nevertheless, ES induced trabecular bone growth around the stimulated implants [40].

Bins-Ely *et al.* (2017) [41] used a beagle dog model and placed commercially pure (cp) Ti grade IV dental implants 2 mm below the crestal bone in the tibia. They applied constant current of 10 and 20 µA for 7 and 15 days, respectively, using an electronic device which was linked to the implant connection area [41]. Their result showed significantly higher BIC after 15 days of stimulation of 20 µA compared to stimulation of 10 µA and control. However, no significant change in BIC was observed among the groups after 7 days.

Furthermore, Buch *et al.* (1984) [12] applied a constant DC current of 5, 20 and 50 µA for 3 weeks in a rabbit model. The implant was placed in between the titanium cathode and platinum-iridium anode in the proximal part of the tibial metaphysis. Bone mineral content (BMC) was significantly higher in 5 and 20 µA specimens compared to 50 µA and controls. However, no qualitative differences between the stimulated groups and the control were found [12]. Infection was not observed and severe inflammatory reaction was absent in all samples, although a black ring was noted around the anodes in the 50 µA group. In all stimulated samples, bone tissue overgrowth of the cathode was noticed [12].

Moreover, Shayesteh *et al.* (2007) [42] provided an EF of 20 µA between two titanium dental implants placed in the mandibular of a mongrel dog. The stimulation was ongoing for 30 days and the implants were evaluated 90 days post-surgery. The authors reported that bone contact ratio (BCR) and local bone formation around the stimulated implants were greater compared to non-stimulated surfaces, but they did not declare if the evaluated implants were cathodes, anodes or both [42].

By utilising a mongrel dog model Colella *et al.* (1981) [43] applied constant DC of 15 µA for 1-8 days in porous titanium cylindrical implants inserted in the mid-diaphysis of the femur. Evaluation was made 1, 2 and 3 weeks post-surgery where a substantially greater maximum shear stress was required to push out the stimulated implants compared to the controls. However, no qualitative difference was detected for the bone ingrowth, but their result implies that ES enhance bone rate and quantity of bone ingrowth since the stimulated implant appeared to adhere more closely to bone than the control [43].

Dergin *et al.* (2013) [8] used a sheep model where they stimulated titanium dental implants placed in the tibia with constant DC current of 7.5 µA for 4, 8 and 12 weeks. The stimulation was ongoing for 12 h per day, 6 h on and 6 h off. No significant increase in BIC ratio, osteoblast activity, or new bone

307 formation was shown in the stimulated implants compared to the control. Furthermore, BEC has also
308 been investigated in a beagle dog model by Song *et al.* (2009) [7]. They stimulated titanium dental
309 implants inserted in the mandible with an amplitude of 20 µA/cm^2, pulse width of 125 µs and a fre-
310 quency of 100 Hz. The stimulation was ongoing for 7 days and the evaluation was performed 3 and 5
311 weeks post-surgery. They reported significant increase in newly formed BA after 3 and 5 weeks com-
312 pared to controls, but only significant increase in BIC stimulated specimens after 3 weeks and no in-
313 crease between stimulated and controls after 5 weeks [7].

314 *Table 3. In vivo* studies categorised in animal model, implant type and material, evaluation, stimulation parameter, stimulation duration and results.
315

Reference	Animal model (implant site)	Implant type & material	Evaluation	Stimulation parameter	Stimulation duration	Results
Isaacson *et al*. 2011 [40]	Rabbit (femur, medullary channel)	Dental implant, Ti6Al4V	SEM[1], histological assessment (bone ingrowth), porosity analysis (mineral apposition rate), biomechanical testing (degree of skeletal attachment was tested with push-out tests)	0.55 V (1.2 V/cm and 1.82 mA/cm^2)	3 and 6 weeks	Significant increase of trabecular bone around the implant in the stimulated group compared to non-stimulated. Slightly higher values for appositional bone index and mineral apposition rates in stimulated groups, although no significant values.
Bins-Ely *et al*. 2017 [41]	Beagle dogs (tibia)	Dental implant, cp Ti grade IV	BIC[2] by histology and histomorphometry analysis	10 µA and 20 µA constant DC[3]	7 and 15 days	Significant increase in BIC after 15 days of stimulation of 20 µA compared to stimulation of 10 µA and control group. No significant results between the groups after 7 days.
Buch *et al*. 1984 [12]	Rabbit (tibial metaphysis)	Cylinder with two chambers, titanium	Histology (qualitative analysis), microradiography followed by a computer-aided density analysis	5 µA, 20 µA and 50 µA constant DC	3 weeks	Significant difference in BMC[4] with stimulation of 5 and 20 µA. No significant difference of BMC with stimulation of 50 µA and no significant difference in qualitative analysis between stimulated and no stimulated groups. The cathode was always overgrown with bone tissue in those cases when it had been connected to the simulator.
Shayesteh *et al*. 2007 [42]	Mongrel dogs (mandible)	Dental implant, titanium	BCA[5] and BCR[6] by histological evaluation, quantitative and qualitative analysis	20 µA, 3V, constant DC	30 days (evaluation after 90 days)	Significant increase in BCR and local bone formation around the stimulated implants as compared to non-stimulated control implants when evaluated at 90 days.
Colella *et al*. 1981 [43]	Mongrel dogs (femur)	Porous cylinder, titanium	SEM (bone-implant interference), EDAX[7] analysis (determine the calcium content within the implants), push-out-test (mechanical testing)	15 µA constant DC	1, 6, 7, 8 days (evaluation after 1, 2 and 3 weeks)	A substantially greater maximum shear stress was needed to push out the stimulated implant as compared to the control. No qualitative difference was detected between the bone in growth in the experimental and control implants. The results imply that ES[8] promote both rate and quantity of bone ingrowth, since stimulated implant did appear to adhere more closely to bone.
Dergin *et al*. 2013 [8]	Sheep (tibia)	Dental implant, titanium	BIC, degree of osteoblast activity, necrosis, immature bone, and mature bone formation by histologic and histomorphometry analysis	7.5 µA constant DC during a period of 12 hours per day (6 h off and 6 h on)	4, 8 and 12 weeks	No significant increase in BIC ratio, osteoblast activity, or new bone formation as compared to non-stimulated controls.
Song *et al*. 2009 [7]	Beagle dogs (mandible)	Dental implant, titanium	BIC and BA[9] by histological evaluations	BEC stimulation with current density of 20 µA/cm^2, pulse width of 125 µs and a frequency of 100 Hz	7 days (evaluation after 3 and 5 weeks)	Significant increase in newly formed bone area after 3 and 5 weeks. Significant increase in BIC in specimen after 3 weeks, no significant difference between stimulated and non-stimulated specimens in BIC after 5 weeks.

[1]**SEM**, scanning electron microscopy; [2]**BIC**, bone-implant contact; [3]**DC**, direct current; [4]**BMC**, bone mineral content; [5]**BCA**, bone contact area; [6]**BCR**, bone contact ratio; [7]**EDAX**, energy dispersion analysis by x-rays; [8]**ES**, electrical stimulation; [9]**BA**, bone area.

The reviewed *in vivo* applications provide more consistent results across studies than the *in vitro* studies. However, it is important to emphasise differences between the study designs, such as animal model used (rabbit, beagle dog, mongrel dog, sheep), location of the implant (medullary channel, tibia, mandible, femur), metal alloy (titanium, Ti6Al4V, cp Ti grade IV), implant type (dental implant, porous cylinder, cylinder with chambers), experimental timeline (stimulation duration relative valuation time point) and applied electrical stimulation (magnitude, pattern, duration, control unit). Despite the protocol differences among *in vivo* studies, there are some recurrent similarities. Both Bins-Ely *et al.* (2017) [41] and Buch *et al.* (1984) [12] investigated different magnitudes of the applied current, 10 and 20 µA and 5, 20 and 50 µA, respectively. Their results showed that there was a clear difference in the outcomes between the applied current, where 10 µA seemed to be to low [41] and 50 µA too high [12] for promoting osseointegration. The observation of a black ring around the anodes by Buch is an indication of cell necrosis, which in turn indicates that it is possible to stimulate with a current magnitude that is too high. This is consistent with the *in vitro* studies [38], [36], [37], [39] that show a voltage/current dependent property for cell viability. Bins-Ely *et al.* (2017) [41] also showed that stimulation duration seems to be an important factor, where no differences between stimulated groups and controls are shown after 7 days, but after 15 days there is a significant difference in BIC between 20 µA compared to the controls.

Studies that analyse bone quality of stimulated versus non-stimulated groups do not observe significant differences [12], [43], but bone quantity in terms of BIC, BA, BCR and BMC has been shown to be significantly greater in the majority of the *in vivo* applications [12], [17], [40]–[43]. When plotting the amplitude against the stimulation duration, see Figure 3, the majority of studies with a significant beneficial outcome can be found in the range between an amplitude of 15-20 µA and stimulation duration between 2-5 weeks. Note that the significant result is focused on bone quantity result and the *in vivo* studies plotted in Figure 3 used a current-controlled stimulation. However, increased bone quantity was not observed in the Dergin *et al.* (2013) [8] sheep model. When

comparing Dergin's study to the *in vivo* applications with statistically significant results, there are three main differences in stimulation parameters, namely: current amplitude, stimulation duration and stimulation treatment. The applied current in the sheep study, 7.5 µA, is below the current limit that previously showed to be too low [41]. Evaluation assessments were performed 4, 8 and 12 weeks post-surgery which is in the late-phase of implant healing; other studies evaluated at an earlier phase [7], [12], [41]–[43] as seen in Figure 3. Dergins' study also stands out when it comes to stimulation treatment; the current is delivered 12 h per day in a pattern of 6 h on and 6 h off, while the other studies delivered a continuous EF through the experiment.

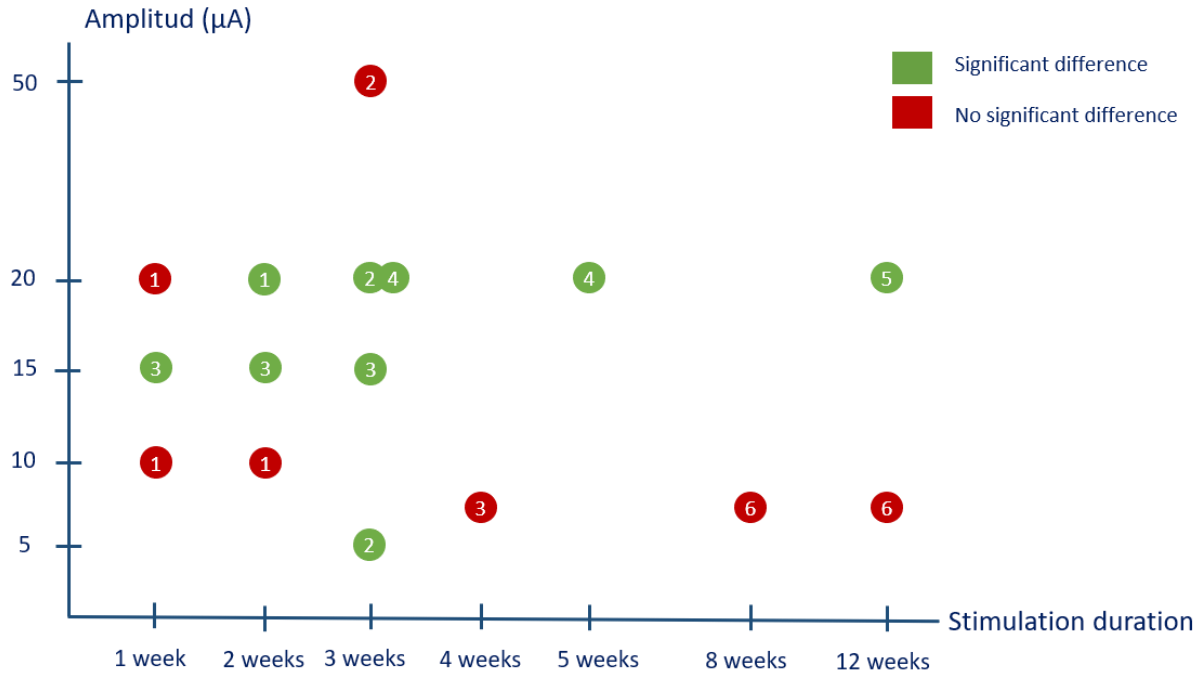

Figure 3: Amplitude vs stimulation duration. Current controlled in vivo studies ***1)*** *Bins-Ely et al. (2017)* [41] ***2)*** *Buch et al. (1984)* [12], ***3)*** *Colella et al. (1981)* [43], ***4)*** *Song ey al. (2009)* [7] ***5)*** *Shayesteh et al. (2007)* [42], ***6)*** *Dergin et al. (2013)* [8]

2 Conclusion

The aim of this review was to compare and contrast published studies that investigated ES as a means to promote osseointegration, with a focus on ES parameters and the use of titanium implants. A total of 13 papers were identified that explored *in vitro* or *in vivo* methods for evaluating the potential effect of ES on osseointegration. These studies utilized a variety of assessments, including

commercially-available assays, that evaluated cell function, viability, and attachment as well as histology and inflammation at the site of implant in animal models. Taken together, *in vitro* models showed that osteoblasts were shown to be sensitive to current/voltage magnitude, stimulation duration as well as the stimulation treatment, likewise for bone quantity around implants in *in vivo* applications.

This review highlights a gap between *in vitro* and *in vivo* studies of ES and osseointegration. For example, *in vitro* studies reported better osseointegration outcomes following stimulation with amplitudes around 15-25 µA. Nevertheless, *in vivo* studies published after these results utilised amplitudes lower than the identified minimum thresholds (e.g., Dergin *et al.* (2013) [8], sheep model). However, it can be difficult to directly translate *in vitro* methods to the *in vivo* setting. The *in vitro* models reviewed here were based on cell culture of one cell line per study. These models are unable to account for bone remodelling (interplay between osteoblast and osteoclast), response from inflammatory cells and the immune system, as well as the role of mechanical stimuli. Thus, for the purpose of evaluating the impact of ES parameters on osseointegration, *in vitro* models can serve as an initial phase to reduce the unnecessary use of animals, but additional optimization is required when translating to *in vivo* study designs. It may be possible to use more complex cell culture models, such as 3D cell cultures [44] or "tissue-in-a-disk" [45] set-ups to better capture 3D interactions in an *in vitro* setting. Some studies also performed additional assays as proxies for *in vivo* effects, such as bone markers for mineralisation. Interestingly, conclusions regarding which ES parameters provided the greatest promotional effect on osseointegration depended on the assessments employed, and most *in vitro* and *in vivo* studies focused on cell viability and proliferation or bone quantity, respectively.

In order to reach a clinically use for DC stimulation there remain some challenges including finding the parameters with most beneficial impact in bone-implant interface as well as further investigating the addressed problems with DC stimulation.

4 List of abbreviations

AC = alternating current

ALP = alkaline phosphate

Au = gold

BA = bone area

BCA = bone contact area

BCR = bone contact ratio

BEC = biphasic electrical current

BIC = bone-implant contact

Bmp2 = bone morphogenetic protein 2

Col I = collagen type 1

DC = direct current

EDAX = energy dispersion analysis by x-rays

EDTA = ethylenediaminetetraacetic acid

EF = electric field

ELISA = enzyme-linked immunosorbent assay

EMF = electromotive force

ES = electrical stimulation

hFOB = human foetal osteoblasts

hmgb1 = high-mobility group box 1

hPOB = human primary osteoblasts

MTT = 3-(4,5-dimethylthiazol-2-yl)-2,5-diphenyltetrazolium bromide

OPG = osteoprotegerin

OC = osteocalcin

Pt = platinum

rcOB = rat calvarial osteoblasts

RNA = ribonucleic acid

RT-PCR = reverse transcription polymerase chain reaction

Runx2 = Runt-related transcription factor 2

SEM = scanning electron microscopy

Spp1 = secreted phosphoprotein 1

Ti = titanium

VEGF = vascular endothelial growth factor

WST-1 = 2-(4-Iodophenyl)-3-(4-nitrophenyl)-5-(2,4-disulfophenyl)-2H-tetrazolium

5 References

[1] P. I. Brånemark *et al.*, 'Osseointegrated implants in the treatment of the edentulous jaw. Experience from a 10-year period', *Scand J Plast Reconstr Surg* , vol. 16, pp. 1–132, 1977.

[2] A. Thesleff, R. Brånemark, B. Håkansson, and M. Ortiz-Catalan, 'Biomechanical Characterisation of Bone-anchored Implant Systems for Amputation Limb Prostheses: A Systematic Review', *Annals of Biomedical Engineering*, vol. 46, no. 3. Springer New York LLC, pp. 377–391, 01-Mar-2018.

[3] K. Pałka and R. Pokrowiecki, 'Porous Titanium Implants: A Review', *Adv. Eng. Mater.*, vol. 20, no. 5, p. 1700648, May 2018.

[4] M. T. Ehrensberger, C. M. Clark, M. K. Canty, and E. P. McDermott, 'Electrochemical methods to enhance osseointegrated prostheses', *Biomed. Eng. Lett.*, 2019.

[5] C. M. Clark, 'Electrochemical Methods for Biofilm Detection and Characterization of Electrically Stimulated Orthopedic Biomaterials', University of Buffalo, State University of New York, 2020.

[6] W. Wang and J. P. Lynch, 'Quantitative assessment of compress-type osseointegrated prosthetic implants in human bone using electromechanical impedance spectroscopic methods', *Biomed. Eng. Lett.*, 2019.

[7] J. K. Song *et al.*, 'An electronic device for accelerating bone formation in tissues surrounding a dental implant', *Bioelectromagnetics*, vol. 30, no. 5, pp. 374–384, 2009.

[8] G. Dergin, M. Akta, B. Gürsoy, Y. Devecioglu, M. Kürkçü, and E. Benlidayi, 'Direct current electric stimulation in implant osseointegration: An experimental animal study with sheep', *J. Oral Implantol.*, vol. 39, no. 6, pp. 671–679, Dec. 2013.

[9] H. S. Alghamdi, 'Methods to improve osseointegration of dental implants in low quality (type-IV) bone: An overview', *Journal of Functional Biomaterials*, vol. 9, no. 1. MDPI AG, 13-Jan-2018.

[10] E. Fukada and I. Yasuda, 'On the Piezoelectric Effect of Bone', *J. Phys. Soc. Japan*, vol. 12, no. 10, pp. 1158–1162, Dec. 1957.

[11] K. Kubota, N. Yoshimura, M. Yokota, R. J. Fitzsimmons, and U. M. E. Wikesjö, 'Overview of Effects of Electrical Stimulation on Osteogenesis and Alveolar Bone', *J. Periodontol.*, vol. 66, no. 1, pp. 2–6, Jan. 1995.

[12] F. Buch, T. Albrektsson, and E. Herbst, 'Direct current influence on bone formation in titanium implants', *Biomaterials*, vol. 5, no. 6, pp. 341–346, 1984.

[13] C. B. Goodwin, C. T. Brighton, R. D. Guyer, J. R. Johnson, K. I. Light, and H. A. Yuan, 'A double-blind study of capacitively coupled electrical stimulation as an adjunct to lumbar spinal fusions', *Spine (Phila. Pa. 1976).*, vol. 24, no. 13, pp. 1349–1357, Jul. 1999.
[14] K. Srirussamee, S. Mobini, N. J. Cassidy, and S. H. Cartmell, 'Direct electrical stimulation enhances osteogenesis by inducing Bmp2 and Spp1 expressions from macrophages and preosteoblasts', *Biotechnol. Bioeng.*, vol. 116, no. 12, pp. 3421–3432, Dec. 2019.
[15] L. C. Kloth, 'Electrical Stimulation Technologies for Wound Healing', *Adv. Wound Care*, vol. 3, no. 2, pp. 81–90, Feb. 2014.
[16] B. M. Isaacson, R. D. Bloebaum, and D. L. William, 'Osseointegrated implant with electrical stimulation', US2010152864A1, 2010.
[17] I. S. Kim *et al.*, 'Biphasic electric current stimulates proliferation and induces VEGF production in osteoblasts', *Biochim. Biophys. Acta - Mol. Cell Res.*, vol. 1763, no. 9, pp. 907–916, 2006.
[18] J. A. Spadaro and R. O. Becker, 'Function of implanted cathodes in electrode-induced bone growth', *Med. Biol. Eng. Comput.*, vol. 17, no. 6, pp. 769–775, Nov. 1979.
[19] B. E. Bax *et al.*, 'Stimulation of osteoclastic bone resorption by hydrogen peroxide', *Biochem. Biophys. Res. Commun.*, vol. 183, no. 3, pp. 1153–1158, Mar. 1992.
[20] W. K. Ramp, L. G. Lenz, and K. K. Kaysinger, 'Medium pH modulates matrix, mineral, and energy metabolism in cultured chick bones and osteoblast-like cells', *Bone Miner.*, vol. 24, no. 1, pp. 59–73, 1994.
[21] K. K. Kaysinger and W. K. Ramp, 'Extracellular pH modulates the activity of cultured human osteoblasts', *J. Cell. Biochem.*, vol. 68, no. 1, pp. 83–89, Jan. 1998.
[22] C. T. Brighton, S. Adler, J. Black, N. Itada, and Z. B. Friedenberg, 'Cathodic oxygen consumption and electrically induced osteogenesis', *CLIN.ORTHOP.*, vol. No. 107, no. 107, pp. 277–282, 1975.
[23] M. Shibuya, 'Vascular Endothelial Growth Factor (VEGF) and Its Receptor (VEGFR) Signaling in Angiogenesis: A Crucial Target for Anti- and Pro-Angiogenic Therapies', *Genes and Cancer*, vol. 2, no. 12, pp. 1097–1105, Dec. 2011.
[24] 'Tetrazolium-based assays for cellular viability: a critical examination of selected parameters affecting formazan production - PubMed'. [Online]. Available: https://pubmed.ncbi.nlm.nih.gov/2021931/. [Accessed: 07-Sep-2020].
[25] T. Mosmann, 'Rapid Colorimetric Assay for Cellular Growth and Survival: Application to Proliferation and Cytotoxicity Assays', 1983.
[26] A. Palmquist, 'A multiscale analytical approach to evaluate osseointegration', *Journal of Materials Science: Materials in Medicine*, vol. 29, no. 5. Springer New York LLC, 01-May-2018.
[27] V. Kuete, O. Karaosmanoğlu, and H. Sivas, 'Anticancer Activities of African Medicinal Spices and Vegetables', *Med. Spices Veg. from Africa Ther. Potential Against Metab. Inflammatory, Infect. Syst. Dis.*, pp. 271–297, 2017.
[28] K. M. Joo *et al.*, 'Development and validation of UPLC method for WST-1 cell viability assay and its application to MCTT HCE^{TM} eye irritation test for colorful substances', *Toxicol. Vitr.*, vol. 60, pp. 412–419, Oct. 2019.
[29] Merck, 'Cell Viability and Proliferation Assays | Sigma-Aldrich'. [Online]. Available: https://www.sigmaaldrich.com/technical-documents/articles/biofiles/cell-viability-and-proliferation.html?gclid=CjwKCAiA-f78BRBbEiwATKRRBIfUjTuHpOiIyjngJ34GHm3AW3ftQ52rBnUKqnclnkVr8Q_DFVJGzhoCGqgQAvD_BwE. [Accessed: 04-Nov-2020].
[30] M. J. Sanderson, I. Smith, I. Parker, and M. D. Bootman, 'Fluorescence microscopy', *Cold Spring Harb. Protoc.*, vol. 2014, no. 10, pp. 1042–1065, Oct. 2014.
[31] J. B. Pawley, *Handbook of biological confocal microscopy: Third edition*. Springer US, 2006.
[32] S. Harbron *et al.*, *Molecular Biology and Biotechnology*, 6th ed. Royal Society of Chemistry, 2015.
[33] Karolinska Institutet, 'Enzymkopplad immunadsorberande analys | Svensk MeSH'. [Online]. Available: https://mesh.kib.ki.se/term/D004797/enzyme-linked-immunosorbent-assay.

[Accessed: 03-Nov-2020].
[34] Karolinska Institutet, 'Radioimmunanalys | Svensk MeSH'. [Online]. Available: https://mesh.kib.ki.se/term/D011863/radioimmunoassay. [Accessed: 03-Nov-2020].
[35] Karolinska Institutet, 'Blotting, Western | Svensk MeSH'. [Online]. Available: https://mesh.kib.ki.se/term/D015153/blotting-western. [Accessed: 03-Nov-2020].
[36] T. J. Dauben, J. Ziebart, T. Bender, S. Zaatreh, B. Kreikemeyer, and R. Bader, 'A Novel in Vitro System for Comparative Analyses of Bone Cells and Bacteria under Electrical Stimulation', *Biomed Res. Int.*, vol. 2016, 2016.
[37] R. A. Gittens *et al.*, 'Electrical Polarization of Titanium Surfaces for the Enhancement of Osteoblast Differentiation', vol. 612, no. August 2012, pp. 599–612, 2013.
[38] S. Bodhak, S. Bose, W. C. Kinsel, and A. Bandyopadhyay, 'Investigation of in vitro bone cell adhesion and proliferation on Ti using direct current stimulation', *Mater. Sci. Eng. C*, vol. 32, no. 8, pp. 2163–2168, Dec. 2012.
[39] S. Sivan, S. Kaul, and J. L. Gilbert, 'The effect of cathodic electrochemical potential of Ti-6Al-4V on cell viability: Voltage threshold and time dependence', *J. Biomed. Mater. Res. - Part B Appl. Biomater.*, vol. 101, no. 8, pp. 1489–1497, 2013.
[40] B. M. Isaacson, L. B. Brunker, A. A. Brown, J. P. Beck, G. L. Burns, and R. D. Bloebaum, 'An evaluation of electrical stimulation for improving periprosthetic attachment', *J. Biomed. Mater. Res. - Part B Appl. Biomater.*, vol. 97 B, no. 1, pp. 190–200, 2011.
[41] L. M. Bins-Ely, E. B. Cordero, J. C. M. Souza, W. Teughels, C. A. M. Benfatti, and R. S. Magini, 'In vivo electrical application on titanium implants stimulating bone formation', *J. Periodontal Res.*, vol. 52, no. 3, pp. 479–484, 2017.
[42] Y. S. Shayesteh *et al.*, 'The Effect of a Constant Electrical Field on Osseointegration after Immediate Implantation in Dog Mandibles : A', 2007.
[43] S. M. Colella, A. G. Miller, R. G. Stang, T. G. Stoebe, and D. M. Spengler, 'Fixation of porous titanium implants in cortical bone enhanced by electrical stimulation', *J. Biomed. Mater. Res.*, vol. 15, no. 1, pp. 37–46, 1981.
[44] A. Lindahl *et al.*, *Cartilage and Bone Regeneration*. 2015.
[45] D. W. Hutmacher, T. B. F. Woodfield, and P. D. Dalton, *Scaffold Design and Fabrication*. 2014.